ing the levels of dynactin 1 protein in SBMA, mRNA levels were determined by *in situ* hybridization in AR-97Q and wild-type mice. Although dynactin 1 mRNA was expressed in virtually all motor neurons in the anterior horn, the expression was markedly repressed in AR-97Q mice (Fig. 4*A*). Moreover, the levels of dynactin 1 mRNA were significantly lower in those motor neurons demonstrating nuclear accumulation of pathogenic AR compared with those without 1C2 nuclear staining (Fig. 4*B*). Real-time quantitative PCR also demonstrated a significant decrease in dynactin 1 mRNA levels in the spinal cords of AR-97Q mice at all disease stages compared with those of wild-types (Fig. 4*C*). The level of dynein heavy chain mRNA was decreased in the advanced stage, but not in the preonset period. The levels of dynein intermediate chain mRNA and dynamitin mRNA were not altered either before or after the onset of motor symptoms.

To investigate the role that diminished levels of dynactin 1 play in neurodegeneration in SBMA, we tested whether overexpression of this protein suppressed the cellular toxicity usually observed in the presence of expanded polyglutamine. In SH-SY5Y cells bearing truncated AR containing an expanded polyglutamine, the level of dynactin 1 was decreased both in mRNA and in protein (Fig. 4*D*,*E*). In this cellular model of SBMA, overexpression of dynactin 1 alleviated cell death exerted by pathogenic AR (Fig. 4*E*).

In SBMA mice, the level of dynactin 1 protein in spinal motor neurons was restored by oral administration of sodium butyrate, an HDAC inhibitor that increases the level of histone acetylation leading to promotion of gene transcription (supplemental Fig. 3, available at www.jneurosci.org as supplemental material) (Minamiyama et al., 2004). Sodium butyrate-mediated upregulation of dynactin 1 also eventually alleviated the neurofilament accumulation in skeletal muscle (supplemental Fig. 3, available at www.jneurosci.org as supplemental material), although this treatment had no influence on the subcellular distribution of pathogenic AR protein (Minamiyama et al., 2004). These observations indicate that nuclear accumulation of aberrant AR in the nuclei of motor neurons leads to a decrease at the transcription level of dynactin 1, resulting in perturbation of retrograde axonal transport and subsequent motor neuron dysfunction.

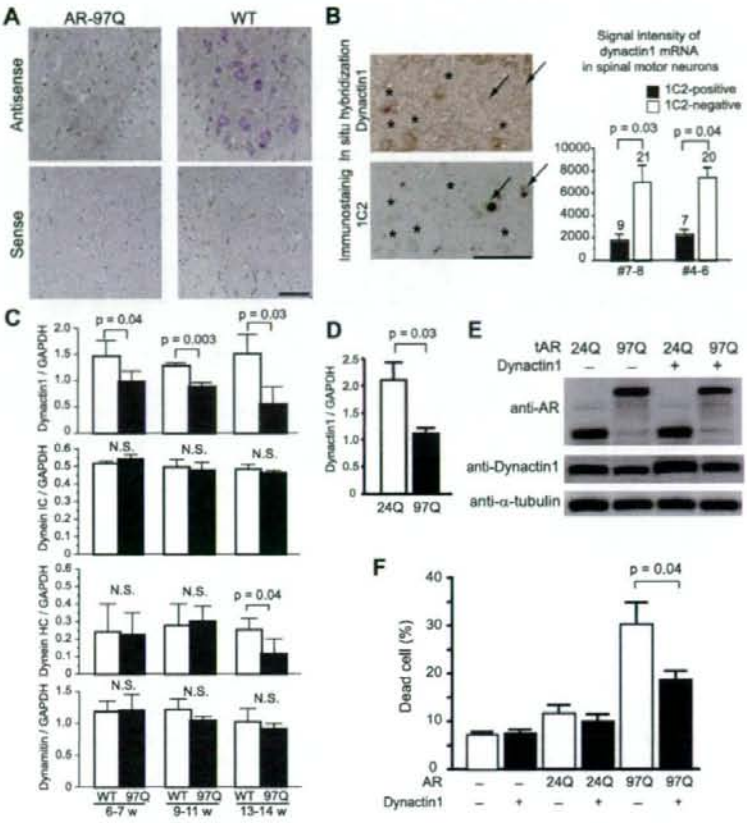

Figure 4. Transcriptional dysregulation of dynactin 1 in spinal motor neurons of SBMA mouse and effects of dynactin 1 overexpression. ***A***, *In situ* hybridization of dynactin 1 mRNA in the anterior horn of wild-type and AR-97 (4–6, 9 weeks) transgenic mice. Note the marked decrease in dynactin 1 mRNA levels in the spinal motor neurons of AR-97Q compared with those in wild-type mice. ***B***, *In situ* hybridization of dynactin 1 in the anterior horn. The adjacent sections were processed for anti-polyglutamine using the 1C2 antibody and the signals were quantified in representative AR-97Q mice (7–8, 9 weeks; 4–6, 10 weeks). Dynactin 1 mRNA expression is markedly decreased in the motor neurons demonstrating nuclear accumulation of pathogenic AR (arrows), but not in those lacking clear nuclear staining with anti-polyglutamine antibody (asterisks). The number above each bar indicates cell count. ***C***, The mRNA levels of dynactin 1 and other motor proteins in the spinal cords of wild-type and AR-97Q mice (7–8, 13 weeks) ($n = 4$ for each group) demonstrated by real-time, RT-PCR. Data shown are ratios of the various mRNA levels to GAPDH mRNA levels. ***D***, The mRNA levels of dynactin 1 in SH-SY5Y cells expressing either AR-24Q or AR-97Q ($n = 4$). ***E***, Immunoblots of SH-SY5Y cells expressing either AR-24Q or AR-97Q with or without overexpression of exogenous dynactin 1. ***F***, Frequency of cell death detected by propidium iodide staining. Dynactin 1 overexpression significantly reduced cell death in the cells bearing AR with elongated polyglutamine. Scale bars: ***A***, ***B***, 100 μm. Error bars indicate SD ($n = 6$ for each group). IC, Intermediate chain; HC, heavy chain.

Castration reverses symptoms and pathology of SBMA mouse

To examine the reversibility of the phenotypes resulting from polyglutamine-induced neuronal dysfunction, we investigated the effect of castration on early symptomatic SBMA mice. Male AR-97Q mice (7–8 and 4–6) demonstrate a rapid aggravation of neuromuscular phenotypes and usually succumb 3–4 weeks after the onset of motor impairment. The motor-impaired phenotype of the SBMA mouse is dependent on circulating testosterone levels, and we reported previously that castration during the presymptomatic period (4 weeks), to eliminate testosterone, drastically prevents the development of neurological symptoms such as weakness, amyotrophy, and shortened life span (Katsuno et al., 2002). In the present study, we castrated male AR-97Q mice within 1 week after the onset of rotarod task impairment. Castration reversed motor dysfunction in AR-97Q mice, even though it was performed after the onset of symptoms (Fig. 5*A*). Most mice showed a reduction in daily activity and body weight loss at the onset of rotarod task defect; these symptoms were also reversed by castration. In accordance with these observations,

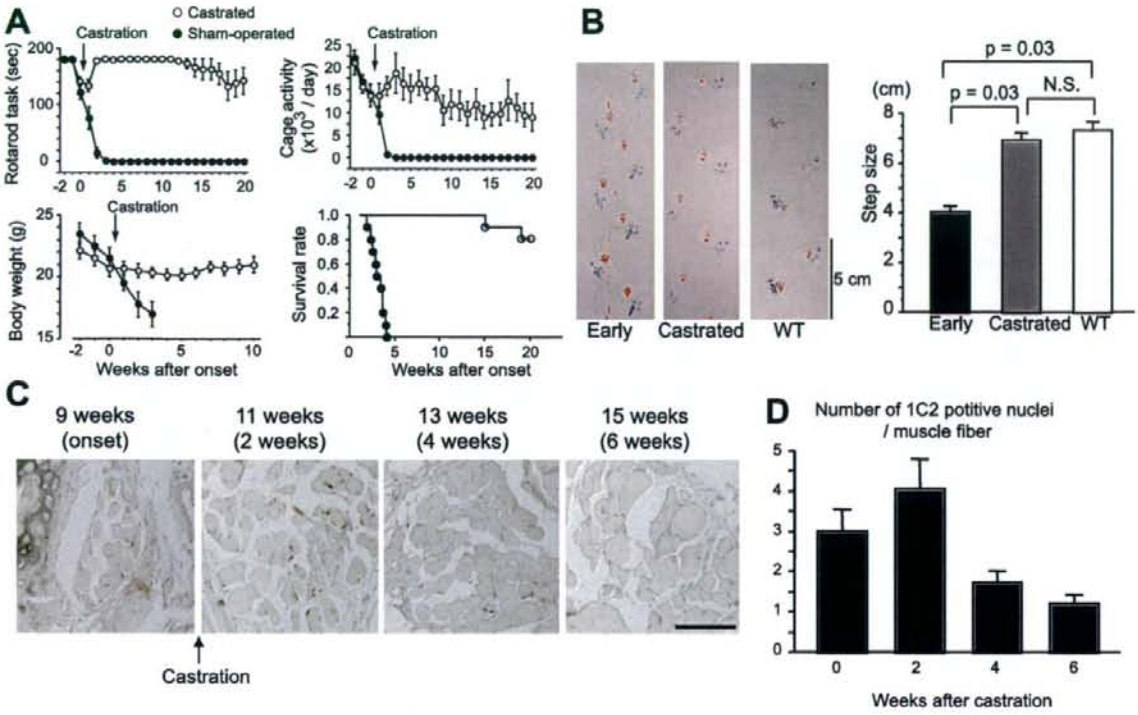

Figure 5. Symptomatic and histopathological reversibility of the SBMA phenotype in AR-97Q mice. ***A***, Castration of early symptomatic AR-97Q mice within 1 week after symptomatic manifestation resulted in significant improvement of the symptomatic phenotypes: rotarod task (7–8), cage activity (4–6), body weight (4–6), and survival rate (4–6). There are significant differences in all parameters between the sham-operated ($n = 10$) and castrated ($n = 10$) male AR-97Q mice ($p < 0.0001$, $p < 0.0001$, $p = 0.0001$, and $p = 0.0006$, respectively). ***B***, Representative footprints of an individual AR-97Q mouse (2–6) at the early onset of motor symptoms and after he had been castrated within 1 week after the onset of rotarod impairment, compared with those of a wild-type mouse. Quantification of the gait stride data ($n = 4$). ***C***, Nuclear accumulation of pathogenic AR with expanded polyglutamine in the tail muscle of one individual male AR-97Q mouse (4–6). ***D***, Castration after motor impairment onset significantly reduced the number of nuclei stained by an anti-polyglutamine antibody, 1C2 ($n = 4$). Scale bar: ***C***, 100 μm. Error bars indicate SD.

postonset castration significantly prolonged the life span of the male AR-97Q mice. We confirmed the reversal of motor symptoms by analyzing gait strides in a series of mouse footsteps (Fig. 5*B*).

To confirm the rescue effects of castration on histopathology, we investigated the nuclear accumulation of pathogenic AR in the skeletal muscle of tail sections sampled over time from the same mouse. Although the number of nuclei positively stained with 1C2 continued to increase for 2 weeks after the castration, at 4 weeks there was a significant decrease in expanded polyglutamine AR-positive nuclei (Fig. 5*C*,*D*). This time course corresponds approximately to the that of the symptomatic improvements, suggesting that nuclear accumulation of pathologic AR contributes to neuronal dysfunction and consequent symptomatic manifestation in SBMA mice.

Castration reverses dynactin 1 expression and restores retrograde axonal transport

It is important to determine whether disrupted retrograde axonal transport resulting from transcriptional dysregulation of dynactin 1, contributes to the reversible motor neuronal dysfunction in the early disease stage of SBMA mice. We therefore investigated axonal transport and the level of dynactin 1 expression in transgenic mice within 1 week after the onset of rotarod task impairment. In this early stage of the disease, the mice already demonstrated a reduction in the number of spinal motor neurons labeled by Fluoro-gold (Fig. 6*A*). Castration of symptomatic AR-97Q mice restored Fluoro-gold staining in the spinal motor neurons to a similar level as seen in wild-types (compare Figs. 2*D*, 6*A*). Castration after the onset of muscle weakness reduced the intramuscular accumulation of neurofilaments and synaptophysin in AR-97Q mice (Fig. 6*B*,*C*). Immunohistochemistry of spinal cord showed that postsymptomatic castration also eliminated nuclear accumulation of pathogenic AR as detected by the 1C2 antibody, and restored anti-dynactin 1 immunoreactivity in motor neurons (Fig. 6*D*). Immunoblotting demonstrated that the level of dynactin 1 protein, but not that of dynein heavy chain, was decreased in the ventral root of AR-97Q mice in the early symptomatic stage (Fig. 6*E*). Castration after the onset of motor impairment restored dynactin 1 to its normal levels in the ventral root, whereas it had no effect on dynactin 1 expression in wild-type mice (Fig. 6*E*). These observations indicate that the castration-mediated restoration of dynactin 1 expression improves retrograde axonal transport and contributes to the reversal of neuromuscular phenotypes in SBMA mice at an early stage of the disease process.

Discussion

Reversibility of neuronal dysfunction in SBMA

The fundamental pathological feature of polyglutamine diseases is the loss of neurons in selected regions of the CNS. Neuronal cell death, however, is often undetectable in mildly affected HD pa-

tients despite the presence of definite clinical features (Vonsattel et al., 1985). The early HD symptoms may thus result from functional alterations within neurons rather than cell death (Walker et al., 1984). In mouse models of polyglutamine diseases, it has been postulated that neuronal dysfunction, without cell loss, is sufficient to cause neurological symptoms (Mangiarini et al., 1996; Clark et al., 1997). These observations indicate that the pathogenesis of polyglutamine diseases is potentially reversible at an early stage. This hypothesis is supported by the observation that arrest of gene expression after the onset of symptoms reverses behavioral and neuropathological abnormalities in conditional mouse models of polyglutamine diseases (Yamamoto et al., 2000; Zu et al., 2004). The present study supports this hypothesis in that castration after the onset of motor deficit reverses behavioral and histopathological abnormalities by preventing nuclear accumulation of the pathogenic AR protein. These findings imply that cellular protective responses successfully abrogate the toxicity of polyglutamine-containing pathogenic protein, unless it perpetually accumulates in the nucleus.

Protein quality control systems, including molecular chaperones, the ubiquitin-proteasome system, and autophagy have been shown to reduce polyglutamine toxicity in various animal models of polyglutamine diseases (Adachi et al., 2003; Ravikumar et al., 2004; Katsuno et al., 2005; Waza et al., 2005). It is thus logical that inhibition of AR translocation into the nucleus restores the protein degradation machinery, such as ubiquitin-proteasome system, leading to the reduction in the amount of aggregates as well as the improvement of neuronal dysfunction in the SBMA mice (Waza et al., 2005).

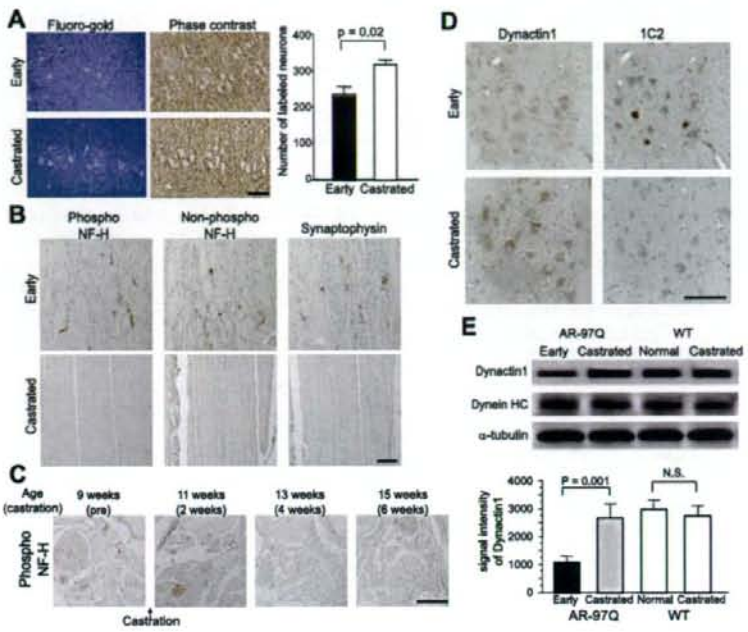

Figure 6. Hormonal intervention restores expression level of dynactin 1 and improves axonal transport. ***A***, Fluoro-gold labeling of spinal cord from early symptomatic (7–8; 9–11 weeks) and castrated (7–8; 13–16 weeks) male AR-97Q mice ($n = 5$ for each group). ***B***, Immunohistochemistry of skeletal muscle for NF-H and synaptophysin. ***C***, Immunohistochemistry for phosphorylated NF-H in the tail muscle of an individual male AR-97Q mouse (4–6). Castration after onset of symptoms depletes NF-H accumulation in the skeletal muscle. ***D***, Immunohistochemistry of the spinal cords of early symptomatic (4–6; 11 weeks) and castrated (4–6; 15 weeks) male AR-97Q mice using anti-dynactin 1 and 1C2. Castration eliminated nuclear accumulation of expanded polyglutamine AR. ***E***, Immunoblots of ventral roots from early symptomatic (4–6; 11 weeks) and castrated (4–6; 15 weeks) AR-97Q mice together with that from wild-type littermates (15 weeks) using antibodies against dynactin 1, dynein heavy chain (HC), and α-tubulin. Scale bars: ***A–D***, 100 μm. Error bars indicate SD ($n = 3$ for each group).

Defective retrograde axonal transport in SBMA

The SBMA mice we examined demonstrated impairment of retrograde axonal transport, resulting in the accumulation of neurofilaments and synaptophysin in the distal motor axon. Many proteins required for neuronal survival are synthesized within neuronal perikarya and are transported along the axon toward the synaptic terminals (Shea, 2000). A bidirectional delivery system consisting of anterograde and retrograde transport enables the recycling of cytoskeletons and synaptic vesicle-associated proteins. A histopathological hallmark of amyotrophic lateral sclerosis (ALS) is the accumulation of neurofilaments in cell bodies and proximal axons of affected motor neurons, presumably caused by compromised anterograde axonal transport; nevertheless, this finding has not been observed in SBMA (Sobue et al., 1990; Julien 2001). Transgenic SBMA mice demonstrate marked neurofilament storage in the distal motor axons, but not in the proximal axons or cell bodies. Neurofilament accumulation at motor endplates has also been reported in a transgenic mouse model of spinal muscular atrophy, another lower motor neuron disease (Cifuentes-Diaz et al., 2002). Axonal transport of NF depends on the dynein/dynactin system, disruption of which results in accumulation of neurofilaments at the distal axon in both cultured cells and transgenic mice (LaMonte et al., 2002; He et al., 2005). When combined, these findings indicate that the accumulation of axonal components in distal motor axons appears to be a substantial pathology associated with degeneration of lower motor neurons.

In the present study, synaptophysin showed an accumulation pattern similar to that of neurofilaments, whereas the distribution of Rab3A, another synaptic vesicle-associated protein, was not altered in this mouse model. Crush injury experiments have shown that although both proteins are delivered from cell bodies into axons, of the two only synaptophysin undergoes retrograde transport (Li et al., 1995, 2000). In addition, Fluoro-gold labeling experiments clearly demonstrated the disruption of retrograde, but not anterograde axonal transport in the spinal motor neurons of SBMA mice before the onset of muscle weakness. Together, the pathogenesis of motor neuronal dysfunction in SBMA is likely to be based on the perturbation of retrograde axonal transport, and not on an excessive transport of total axonal proteins.

Axonal transport impairment has been implicated in the pathogenesis of HD and SBMA (Gunawardena et al., 2003; Szebenyi et al., 2003). Although axonal inclusion interferes with axonal transport in a cell model of SBMA (Piccioni et al., 2002), AR containing expanded polyglutamine may also inhibit anterograde and/or retrograde axonal transport without visible aggregate formation (Szebenyi et al., 2003; Morfini et al., 2006). Accu-

mulation of neurofilaments at nerve terminals has also been documented in a mouse model of HD (Ribchester et al., 2004). In our SBMA mice, pathogenic AR did not colocalize with accumulated neurofilament, nor did it form axonal inclusions. More intriguingly, sodium butyrate-mediated gene upregulation attenuated the accumulation of neurofilaments, but did not alter the intracellular distribution of AR. These observations suggest that the defective retrograde axonal transport in SBMA mice does not result from the direct interaction between aberrant AR and axonal components, but rather from a secondary mechanism resulting from expanded polyglutamine.

Dynactin in motor neuron disease

The present study indicates that a decrease in the level of dynactin 1, the p150 subunit of dynactin, in affected neurons is a fundamental early event in the pathogenesis of SBMA. Dynactin is a multiprotein complex regulating dynein, a microtubule-dependent molecular motor for retrograde axonal transport. A mutation in *DCTN1*, the gene encoding dynactin 1, has been identified in a family with an autosomal dominant form of lower motor neuron disease and in another with ALS (Puls et al., 2003; Münch et al., 2005). A gene expression analysis of sporadic ALS patients revealed a significant decrease in dynactin 1 mRNA (Jiang et al., 2005). Overexpression of dynamitin dissociates the dynactin complex, resulting in late-onset motor neuron degeneration in a transgenic mouse model of motor neuron disease (LaMonte et al., 2002). These observations specifically link an impaired dynactin function to the pathogenesis of motor neuron diseases.

The pathological alteration in individual polyglutamine diseases is limited to distinct subsets of neurons, suggesting that the causative protein context influences the distribution of lesions. Motor neurons are selectively affected in SBMA, although pathogenic ARs are expressed in a wide range of neuronal and non-neuronal tissues (Doyu et al., 1994). A decreased level of dynactin 1 may contribute to this pathological selectivity, because a mutation in the *DCTN1* gene causes a lower motor neuron disease resembling SBMA (Puls et al., 2003, 2005).

Link between altered transcription and neuronal dysfunction

Numerous studies have shown that nuclear accumulation of pathogenic polyglutamine-proteins is essential for neurodegeneration, although cytoplasmic events may also contribute to the pathogenesis (Gatchel and Zoghbi, 2005). Polyglutamine aggregation sequesters a variety of fundamental cellular factors including heat shock proteins and proteasomal components as well as transcriptional factors and coactivators. cAMP response element-binding protein-binding protein (CBP), a transcriptional coactivator, colocalizes with intranuclear inclusions in SBMA patients as well as in transgenic SBMA mice (McCampbell et al., 2000; Nucifora et al., 2001). In addition to its sequestration in inclusion bodies, the histone acetyltransferase activity of CBP is also inhibited by soluble polyglutamine-protein (Steffan et al., 2001). This theory suggests that HDAC inhibitors, which upregulate transcription through acetylation of nuclear histone, may open new avenues in the development of therapeutics. In a fly model of HD, the HDAC inhibitors, sodium butyrate and suberoylanilide hydroxamic acid, increased histone acetylation, leading to the mitigation of neurodegeneration (Steffan et al., 2001). These compounds also improve motor dysfunction in mouse models of HD and SBMA (Hockly et al., 2003; Minamiyama et al., 2004).

In the present study, a reduction in the level of dynactin 1 protein is ascribed to polyglutamine-mediated transcriptional dysregulation, because the mRNA level of this protein is decreased in expanded polyglutamine AR-positive spinal motor neurons. It should be noted that this diminution was significant in the neurons demonstrating nuclear accumulation of pathogenic AR, implying that polyglutamine-induced transcriptional perturbation underlies this pathological process. This hypothesis is confirmed by the observation that administration of sodium butyrate, an HDAC inhibitor, restores dynactin 1 expression, resulting in elimination of neurofilament accumulation at distal motor axons. Although, because of the nonspecific nature of sodium butyrate, we cannot at this time rule out the possibility that expression of some other protein was also elevated, leading to the elimination of neurofilament accumulation.

Given that the expression of other axon motor proteins regulating retrograde axonal transport, such as dynein intermediate chain, dynein heavy chain and dynamitin are not altered before the onset of symptoms, the reduction in dynactin 1 appears to instigate the neurodegeneration in SBMA. In addition to our study, the selective perturbation of certain subsets of gene transcription has been demonstrated in other animal models of polyglutamine diseases (Sugars and Rubinsztein 2003; Sopher et al., 2004), although the precise mechanism has yet to be elucidated.

In summary, the present study demonstrates that the pathogenesis of SBMA is a reversible dysfunction of motor neurons that occurs in the early stages of the disease. Polyglutamine-induced transcriptional alteration of dynactin 1 appears to disrupt retrograde axonal transport, contributing to the early reversible neuronal dysfunction. These observations suggest that transcriptional alteration and subsequent involvement of retrograde axonal transport are substantial therapeutic targets for SBMA.

References

Adachi H, Katsuno M, Minamiyama M, Sang C, Pagoulatos G, Angelidis C, Kusakabe M, Yoshiki A, Kobayashi Y, Doyu M, Sobue G (2003) Heat shock protein 70 chaperone overexpression ameliorates phenotypes of the spinal and bulbar muscular atrophy transgenic mouse model by reducing nuclear-localized mutant androgen receptor protein. J Neurosci 23:2203–2211.

Adachi H, Katsuno M, Minamiyama M, Waza M, Sang C, Nakagomi Y, Kobayashi Y, Tanaka F, Doyu M, Inukai A, Yoshida M, Hashizume Y, Sobue G (2005) Widespread nuclear and cytoplasmic accumulation of mutant androgen receptor in SBMA patients. Brain 128:659–670.

Ando Y, Liang Y, Ishigaki S, Niwa J, Jiang Y, Kobayashi Y, Yamamoto M, Doyu M, Sobue G (2003) Caspase-1 and -3 mRNAs are differentially upregulated in motor neurons and glial cells in mutant SOD1 transgenic mouse spinal cord: a study using laser microdissection and real-time RT-PCR. Neurochem Res 28:839–846.

Banno H, Adachi H, Katsuno M, Suzuki K, Atsuta N, Watanabe H, Tanaka F, Doyu M, Sobue G (2006) Mutant androgen receptor accumulation in spinal and bulbar muscular atrophy scrotal skin: a pathogenic marker. Ann Neurol 59:520–526.

Cha JH (2000) Transcriptional dysregulation in Huntington's disease. Trends Neurosci 23:387–392.

Chevalier-Larsen ES, O'Brien CJ, Wang H, Jenkins SC, Holder L, Lieberman AP, Merry DE (2004) Castration restores function and neurofilament alterations of aged symptomatic males in a transgenic mouse model of spinal and bulbar muscular atrophy. J Neurosci 24:4778–4786.

Cifuentes-Díaz C, Nicole S, Velasco ME, Borra-Cebrian C, Panozzo C, Frugier T, Millet G, Roblot N, Joshi V, Melki J (2002) Neurofilament accumulation at the motor endplate and lack of axonal sprouting in a spinal muscular atrophy mouse model. Hum Mol Genet 11:1439–1447.

Clark HB, Burright EN, Yunis WS, Larson S, Wilcox C, Hartman B, Matilla A, Zoghbi HY, Orr HT (1997) Purkinje cell expression of a mutant allele of

SCA1 in transgenic mice leads to disparate effects on motor behaviors, followed by a progressive cerebellar dysfunction and histological alterations. J Neurosci 17:7385–7395.

Doyu M, Sobue G, Kimata K, Yamamoto K, Mitsuma T (1994) Androgen receptor mRNA with increased size of tandem CAG repeat is widely expressed in the neural and nonneural tissues of X-linked recessive bulbospinal neuronopathy. J Neurol Sci 127:43–47.

Gatchel JR, Zoghbi HY (2005) Diseases of unstable repeat expansion: mechanism and principles. Nat Rev Genet 6:743–755.

Gunawardena S, Her LS, Brusch RG, Laymon RA, Niesman IR, Gordesky-Gold B, Sintasath L, Bonini NM, Goldstein LS (2003) Disruption of axonal transport by loss of huntingtin or expression of pathogenic polyglutamine proteins in *Drosophila*. Neuron 40:25–40.

He Y, Francis F, Myers KA, Yu W, Black MM, Baas PW (2005) Role of cytoplasmic dynein in the axonal transport of microtubules and neurofilaments. J Cell Biol 168:697–703.

Hockly E, Richon VM, Woodman B, Smith DL, Zhou X, Rosa E, Sathasivam K, Ghazi-Noori S, Mahal A, Lowden PA, Steffan JS, Marsh JL, Thompson LM, Lewis CM, Marks PA, Bates GP (2003) Suberoylanilide hydroxamic acid, a histone deacetylase inhibitor, ameliorates motor deficits in a mouse model of Huntington's disease. Proc Natl Acad Sci USA 100:2041–2046.

Ishigaki S, Liang Y, Yamamoto M, Niwa J, Ando Y, Yoshihara T, Takeuchi H, Doyu M, Sobue G (2002) X-linked inhibitor of apoptosis protein is involved in mutant SOD1-mediated neuronal degeneration. J Neurochem 82:576–584.

Jiang YM, Yamamoto M, Kobayashi Y, Yoshihara T, Liang Y, Terao S, Takeuchi H, Ishigaki S, Katsuno M, Adachi H, Niwa J, Tanaka F, Doyu M, Yoshida M, Hashizume Y, Sobue G (2005) Gene expression profile of spinal motor neurons in sporadic amyotrophic lateral sclerosis. Ann Neurol 57:236–251.

Julien JP (2001) Amyotrophic lateral sclerosis: unfolding the toxicity of the misfolded. Cell 104:581–591.

Katsuno M, Adachi H, Kume A, Li M, Nakagomi Y, Niwa H, Sang C, Kobayashi Y, Doyu M, Sobue G (2002) Testosterone reduction prevents phenotypic expression in a transgenic mouse model of spinal and bulbar muscular atrophy. Neuron 35:843–854.

Katsuno M, Adachi H, Doyu M, Minamiyama M, Sang C, Kobayashi Y, Inukai A, Sobue G (2003) Leuprorelin rescues polyglutamine-dependent phenotypes in a transgenic mouse model of spinal and bulbar muscular atrophy. Nat Med 9:768–773.

Katsuno M, Sang C, Adachi H, Minamiyama M, Waza M, Tanaka F, Doyu M, Sobue G (2005) Pharmacological induction of heat-shock proteins alleviates polyglutamine-mediated motor neuron disease. Proc Natl Acad Sci USA 102:16801–16806.

Katsuno M, Adachi H, Waza M, Banno H, Suzuki K, Tanaka F, Doyu M, Sobue G (2006) Pathogenesis, animal models and therapeutics in spinal and bulbar muscular atrophy (SBMA). Exp Neurol 200:8–18.

Kennedy WR, Alter M, Sung JH (1968) Progressive proximal spinal and bulbar muscular atrophy of late onset. A sex-linked recessive trait. Neurology 18:671–680.

Kobayashi Y, Kume A, Li M, Doyu M, Hata M, Ohtsuka K, Sobue G (2000) Chaperones Hsp70 and Hsp40 suppress aggregate formation and apoptosis in cultured neuronal cells expressing truncated androgen receptor protein with expanded polyglutamine tract. J Biol Chem 275:8772–8778.

LaMonte BH, Wallace KE, Holloway BA, Shelly SS, Ascano J, Tokito M, Van Winkle T, Howland DS, Holzbaur EL (2002) Disruption of dynein/dynactin inhibits axonal transport in motor neurons causing late-onset progressive degeneration. Neuron 34:715–727.

La Spada AR, Wilson EM, Lubahn DB, Harding AE, Fischbeck KH (1991) Androgen receptor gene mutations in X-linked spinal and bulbar muscular atrophy. Nature 352:77–79.

Li JY, Jahn R, Dahlstrom A (1995) Rab3a, a small GTP-binding protein, undergoes fast anterograde transport but not retrograde transport in neurons. Eur J Cell Biol 67:297–307.

Li JY, Pfister KK, Brady ST, Dahlstrom A (2000) Cytoplasmic dynein conversion at a crush injury in rat peripheral axons. J Neurosci Res 61:151–161.

Mangiarini L, Sathasivam K, Seller M, Cozens B, Harper A, Hetherington C, Lawton M, Trottier Y, Lehrach H, Davies SW, Bates GP (1996) Exon 1 of the HD gene with an expanded CAG repeat is sufficient to cause a progressive neurological phenotype in transgenic mice. Cell 87:493–506.

McCampbell A, Taylor JP, Taye AA, Robitschek J, Li M, Walcott J, Merry D, Chai Y, Paulson H, Sobue G, Fischbeck KH (2000) CREB-binding protein sequestration by expanded polyglutamine. Hum Mol Genet 9:2197–2202.

Minamiyama M, Katsuno M, Adachi H, Waza M, Sang C, Kobayashi Y, Tanaka F, Doyu M, Inukai A, Sobue G (2004) Sodium butyrate ameliorates phenotypic expression in a transgenic mouse model of spinal and bulbar muscular atrophy. Hum Mol Genet 13:1183–1192.

Morfini G, Pigino G, Szebenyi G, You Y, Pollema S, Brady ST (2006) JNK mediates pathogenic effects of polyglutamine-expanded androgen receptor on fast axonal transport. Nat Neurosci 9:907–916.

Münch C, Rosenbohm A, Sperfeld AD, Uttner I, Reske S, Krause BJ, Sedlmeier R, Meyer T, Hanemann CO, Stumm G, Ludolph AC (2005) Heterozygous R1101K mutation of the DCTN1 gene in a family with ALS and FTD. Ann Neurol 58:777–780.

Niwa H, Yamamura K, Miyazaki J (1991) Efficient selection for high-expression transfectants with a novel eukaryotic vector. Gene 108:193–199.

Nucifora Jr FC, Sasaki M, Peters MF, Huang H, Cooper JK, Yamada M, Takahashi H, Tsuji S, Troncoso J, Dawson VL, Dawson TM, Ross CA (2001) Interference by huntingtin and atrophin-1 with cbp-mediated transcription leading to cellular toxicity. Science 291:2423–2428.

Piccioni F, Pinton P, Simeoni S, Pozzi P, Fascio U, Vismara G, Martini L, Rizzuto R, Poletti A (2002) Androgen receptor with elongated polyglutamine tract forms aggregates that alter axonal trafficking and mitochondrial distribution in motor neuronal processes. FASEB J 16:1418–1420.

Puls I, Jonnakuty C, LaMonte BH, Holzbaur EL, Tokito M, Mann E, Floeter MK, Bidus K, Drayna D, Oh SJ, Brown Jr RH, Ludlow CL, Fischbeck KH (2003) Mutant dynactin in motor neuron disease. Nat Genet 33:455–456.

Puls I, Oh SJ, Sumner CJ, Wallace KE, Floeter MK, Mann EA, Kennedy WR, Wendelschafer-Crabb G, Vortmeyer A, Powers R, Finnegan K, Holzbaur EL, Fischbeck KH, Ludlow CL (2005) Distal spinal and bulbar muscular atrophy caused by dynactin mutation. Ann Neurol 57:687–694.

Ravikumar B, Vacher C, Berger Z, Davies JE, Luo S, Oroz LG, Scaravilli F, Easton DF, Duden R, O'Kane CJ, Rubinsztein DC (2004) Inhibition of mTOR induces autophagy and reduces toxicity of polyglutamine expansions in fly and mouse models of Huntington disease. Nat Genet 36:585–595.

Ribchester RR, Thomson D, Wood NI, Hinks T, Gillingwater TH, Wishart TM, Court FA, Morton AJ (2004) Progressive abnormalities in skeletal muscle and neuromuscular junctions of transgenic mice expressing the Huntington's disease mutation. Eur J Neurosci 20:3092–3114.

Roy S, Coffee P, Smith G, Liem RK, Brady ST, Black MM (2000) Neurofilaments are transported rapidly but intermittently in axons: implications for slow axonal transport. J Neurosci 20:6849–6861.

Sagot Y, Rosse T, Vejsada R, Perrelet D, Kato AC (1998) Differential effects of neurotrophic factors on motoneuron retrograde labeling in a murine model of motoneuron disease. J Neurosci 18:1132–1141.

Schmidt BJ, Greenberg CR, Allingham-Hawkins DJ, Spriggs EL (2002) Expression of X-linked bulbospinal muscular atrophy (Kennedy disease) in two homozygous women. Neurology 59:770–772.

Shea TB (2000) Microtubule motors, phosphorylation and axonal transport of neurofilaments. J Neurocytol 29:873–887.

Sobue G, Hashizume Y, Mukai E, Hirayama M, Mitsuma T, Takahashi A (1989) X-linked recessive bulbospinal neuronopathy. A clinicopathological study. Brain 112:209–232.

Sobue G, Hashizume Y, Yasuda T, Mukai E, Kumagai T, Mitsuma T, Trojanowski JQ (1990) Phosphorylated high molecular weight neurofilament protein in lower motor neurons in amyotrophic lateral sclerosis and other neurodegenerative diseases involving ventral horn cells. Acta Neuropathol (Berl) 79:402–408.

Sopher BL, Thomas Jr PS, LaFevre-Bernt MA, Holm IE, Wilke SA, Ware CB, Jin LW, Libby RT, Ellerby LM, La Spada AR (2004) Androgen receptor YAC transgenic mice recapitulate SBMA motor neuronopathy and implicate VEGF164 in the motor neuron degeneration. Neuron 41:687–699.

Steffan JS, Bodai L, Pallos J, Poelman M, McCampbell A, Apostol BL, Kazant-

sev A, Schmidt E, Zhu YZ, Greenwald M, Kurokawa R, Housman DE, Jackson GR, Marsh JL, Thompson LM (2001) Histone deacetylase inhibitors arrest polyglutamine-dependent neurodegeneration in *Drosophila*. Nature 413:739–743.

Sugars KL, Rubinsztein DC (2003) Transcriptional abnormalities in Huntington disease. Trends Genet 19:233–238.

Szebenyi G, Morfini GA, Babcock A, Gould M, Selkoe K, Stenoien DL, Young M, Faber PW, MacDonald ME, McPhaul MJ, Brady ST (2003) Neuropathogenic forms of huntingtin and androgen receptor inhibit fast axonal transport. Neuron 40:41–52.

Vonsattel JP, Myers RH, Stevens TJ, Ferrante RJ, Bird ED, Richardson Jr EP (1985) Neuropathological classification of Huntington's disease. J Neuropathol Exp Neurol 44:559–577.

Walker FO, Young AB, Penney JB, Dovorini-Zis K, Shoulson I (1984) Benzodiazepine and GABA receptors in early Huntington's disease. Neurology 34:1237–1240.

Waza M, Adachi H, Katsuno M, Minamiyama M, Sang C, Tanaka F, Inukai A, Doyu M, Sobue G (2005) 17-AAG, an Hsp90 inhibitor, ameliorates polyglutamine-mediated motor neuron degeneration. Nat Med 11:1088–1095.

Yamamoto A, Lucas JJ, Hen R (2000) Reversal of neuropathology and motor dysfunction in a conditional model of Huntington's disease. Cell 101:57–66.

Zu T, Duvick LA, Kaytor MD, Berlinger MS, Zoghbi HY, Clark HB, Orr HT (2004) Recovery from polyglutamine-induced neurodegeneration in conditional SCA1 transgenic mice. J Neurosci 24:8853–8861.

doi:10.1093/brain/awl096 Brain (2006), 129, 1446–1455

Natural history of spinal and bulbar muscular atrophy (SBMA): a study of 223 Japanese patients

Naoki Atsuta,[1] Hirohisa Watanabe,[1] Mizuki Ito,[1] Haruhiko Banno,[1] Keisuke Suzuki,[1] Masahisa Katsuno,[1] Fumiaki Tanaka,[1] Akiko Tamakoshi[2] and Gen Sobue[1]

Departments of [1]Neurology and [2]Preventive Medicine/Biostatistics and Medical Decision Making, Nagoya University Graduate School of Medicine, Nagoya, Japan

Correspondence to: Gen Sobue, MD, Department of Neurology, Nagoya University Graduate School of Medicine, Nagoya 466-8550, Japan
E-mail: sobueg@med.nagoya-u.ac.jp

Spinal and bulbar muscular atrophy (SBMA) is an adult-onset motoneuron disease caused by a CAG-repeat expansion in the androgen receptor (*AR*) gene and for which no curative therapy exists. However, since recent research may provide opportunities for medical treatment, information concerning the natural history of SBMA would be beneficial in planning future clinical trials. We investigated the natural course of SBMA as assessed by nine activities of daily living (ADL) milestones in 223 Japanese SBMA patients (mean age at data collection = 55.2 years; range = 30–87 years) followed from 1 to 20 years. All the patients were diagnosed by genetic analysis. Hand tremor was an early event that was noticed at a median age of 33 years. Muscular weakness occurred predominantly in the lower limbs, and was noticed at a median age of 44 years, followed by the requirement of a handrail to ascend stairs at 49, dysarthria at 50, dysphagia at 54, use of a cane at 59 and a wheelchair at 61 years. Twenty-one of the patients developed pneumonia at a median age of 62 and 15 of them died at a median age of 65 years. The most common cause of death in these cases was pneumonia and respiratory failure. The ages at onset of each ADL milestone were strongly correlated with the length of CAG repeats in the *AR* gene. However CAG-repeat length did not correlate with the time intervals between each ADL milestone, suggesting that although the onset age of each ADL milestone depends on the CAG-repeat length in the *AR* gene, the rate of disease progression does not. The levels of serum testosterone, an important triggering factor for polyglutamine-mediated motoneuron degeneration, were maintained at relatively high levels even at advanced ages. These results provide beneficial information for future clinical therapeutic trials, although further detailed prospective studies are also needed.

Keywords: natural history; motoneuron disease; SBMA; Kennedy disease; ADL milestone

Abbreviations: ADL = activities of daily living; ALT = alanine aminotransferase; AR = androgen receptor; AST = aspartate aminotransferase; CK = creatine kinase; HbA1c = haemoglobin A1c; SBMA = spinal and bulbar muscular atrophy

Received January 11, 2006. Revised March 19, 2006. Accepted March 23, 2006. Advance Access publication April 18, 2006

Introduction

Spinal and bulbar muscular atrophy (SBMA) is a neurodegenerative disorder of motoneurons characterized by proximal limb muscular atrophy, bulbar involvement, marked contraction fasciculation, hand tremor and gynaecomastia (Kennedy *et al.*, 1968; Sobue *et al.*, 1989). SBMA is caused by a CAG-repeat expansion in the first exon of the androgen receptor (*AR*) gene on the X-chromosome (La Spada *et al.*, 1991). Similar to other triplet repeat diseases, the age at onset of disease has been inversely linked to the size of the CAG-repeat expansions (Andrew *et al.*, 1993; Sasaki *et al.*, 1996; Rosenblatt *et al.*, 2003). For example, an association between the age at onset of limb muscle weakness and the CAG-repeat length has been demonstrated (Doyu *et al.*, 1992; Igarashi *et al.*, 1992; La Spada *et al.*, 1992; Shimada *et al.*, 1995; Sinnreich *et al.*, 2004). Nuclear accumulation of mutant *AR* with expanded polyglutamines in motoneurons, as well as in other cells, has been shown to be a major pathogenic process (Li *et al.*, 1998*a*, *b*; Adachi *et al.*, 2005). However, the progression and prognosis of SBMA has not been assessed in detail, particularly concerning the influence of CAG-repeat size, the decline of the activities of daily living (ADL) with disease progression and the determination of functional

prognosis. Some SBMA studies reported no correlation between the progression of the clinical course and the number of CAG repeats (Lund *et al.*, 2001; Sperfeld *et al.*, 2002), while other studies revealed an age-assessed severity of limb-muscle weakness (Doyu *et al.*, 1992) or only a weak correlation between the decline of ADL and CAG-repeat expansion (La Spada *et al.*, 1992). Since most of the studies performed thus far contained small sample sizes, the influence of CAG-repeat length on the clinical course of SBMA patients remains obscure. In other CAG-repeat diseases such as Huntington's disease, spinocerebellar ataxia type 3 (SCA3) and dentatorubral-pallidoluysian atrophy (DRPLA), an age-assessed residual cell population, a variety of clinical manifestations and MRI-assessed cerebellar volume have been reported to correlate with CAG-repeat length (Koide *et al.*, 1994; Furtado *et al.*, 1996; Penney *et al.*, 1997; Abe *et al.*, 1998). However, it is still not known how CAG-repeat length influences the progression and prognosis of CAG-repeat diseases.

Recent research has suggested therapeutic approaches to SBMA. In a transgenic mouse model expressing the human *AR* gene with expanded CAG repeats, progressive muscular atrophy and weakness associated with the nuclear accumulation of mutant AR protein was observed. These phenotypes were significantly ameliorated by anti-testosterone therapy (Katsuno *et al.*, 2002, 2003), and the clinical and pathological phenotypes of these mice were markedly improved by the overexpression of heat shock proteins (Adachi *et al.*, 2003; Katsuno *et al.*, 2005). Furthermore, 17-allylamino-17-demethoxygeldanamycin (17-AAG), a potent HSP90 inhibitor, was recently shown to ameliorate motor function deficits and pathological changes in SBMA transgenic mice (Waza *et al.*, 2005). These remarkable therapeutic effects in the transgenic mouse model strongly suggest the possibility of using these approaches in human clinical trials. In order to prepare for such a therapeutic approach, it is important to establish the natural history of clinical symptoms of SBMA based on a large number of patients.

In the present study, we investigated the natural course of SBMA as assessed by 9 ADL milestones in 223 Japanese SBMA patients, and correlated the age of onset of specific milestones during the course of the disease with the CAG-repeat length in the *AR* gene.

Patients and methods

Patients and clinical evaluations

Our laboratory diagnosed 303 patients as SBMA by genetic analysis between 1992 and 2004. Two-thirds of the patients were followed in Nagoya University Hospital or affiliated hospitals, while the other patients were from other hospitals nationwide. These patients were followed by neurologists from 1 year to >20 years. We reviewed the clinical course of the disease in 223 out of 303 patients. The initial symptoms and onset of nine ADL milestones were assessed to evaluate the clinical course of the disease. The ADL milestones were defined as follows: hand tremor (patient awareness of hand tremor), muscular weakness (initial patient awareness of muscular weakness in any part of the body), requirement of a handrail (patient was unable to ascend stairs without the use of a handrail), dysarthria (patient was unable to articulate properly and had intelligible speech only with repetition), dysphagia (patient choked occasionally at meals), use of a cane (patient used a cane constantly when away from home), use of a wheelchair (patient used a wheelchair when away from home) and development of pneumonia (patient developed pneumonia that required in-hospital care). The age at death and cause of death were also investigated. We assessed the age at which the ADL milestones first occurred and the age at death by direct interview, examination of the patients, family interviews and by reviewing the patient's clinical record. The milestones that could be recognized by family members, such as the use of a cane, the use of a wheelchair or the development of pneumonia, were confirmed by them wherever possible.

All evaluators used similar criteria to assess each milestone. To verify these nine ADL milestones as characteristic landmarks in the progression of SBMA symptoms, two neurologists independently assessed their onset in SBMA patients. The accordance between the evaluators of the age of onset of each ADL milestone was verified in 20 SBMA patients with Pearson's correlation coefficients ranging from 0.95 to 0.99.

The clinical landmarks adopted in the previous studies that showed clinical courses of SBMA, based on the characteristic symptoms, were onset of weakness, difficulty climbing stairs, being wheelchair-bound, tremor, gynaecomastia, fasciculations, premature exhaustion of muscles and chewing, muscle cramps, muscle pain, dysarthria and dysphagia (Doyu *et al.*, 1992; La Spada *et al.*, 1992; Shimada *et al.*, 1995; Sperfeld *et al.*, 2002; Sinnreich *et al.*, 2004). We excluded development of gynaecomastia and fasciculation from the ADL milestones, since more than one-third of the patients were not aware of these symptoms, despite their presence. The appearance of muscle cramp and exhaustion of muscles and chewing were also excluded as their recognition was extremely variable among the patients. Some patients recognized them at a very early phase, while others did so only at later stages or not at all.

We used the modified Rankin scale (van Swieten *et al.*, 1988) for the assessment of clinical disability in daily life and examined the serum levels of creatine kinase (CK), aspartate aminotransferase (AST), alanine aminotransferase (ALT), total cholesterol, total testosterone and haemoglobin A1c (HbA1c) as laboratory markers for disease status. As controls, we used the serum levels of CK, AST, ALT, total cholesterol and HbA1c from health screening data of 62–70 males aged 24–79 years, free from neuromuscular diseases. For serum testosterone levels, we adopted published control data from 1143 Japanese males determined by the same assay method that we used in this study (Iwamoto *et al.*, 2004).

We implemented the ethics guideline for human genome/gene analysis research and the ethics guideline for epidemiological studies endorsed by the Japanese government. Before we interviewed the patients, we obtained written informed consent. In cases where this was not possible, such as deceased patients, we used only existing material without informed consent and strictly protected anonymity. All of the study plans were approved by the ethics committee of Nagoya University Graduate School of Medicine.

Genetic analysis

Genomic DNA was extracted from peripheral blood of the SBMA patients using conventional techniques. PCR amplification of the

CAG repeat in the *AR* gene was performed using a fluorescein-labelled forward primer (5′-TCCAGAATCTGTTCCAGAGCGT-GC-3′) and a non-labelled reverse primer (5′-TGGCCTCGCTCAG-GATGTCTTTAAG-3′). Detailed PCR conditions were described previously (Tanaka *et al.*, 1999). Aliquots of PCR products were combined with loading dye and separated by electrophoresis with an autoread sequencer SQ-5500 (Hitachi Electronics Engineering, Tokyo, Japan). The size of the CAG repeat was analysed on Fraglys software version 2.2 (Hitachi) by comparison with co-electrophoresed PCR standards with known repeat sizes. The CAG-repeat size of the PCR standard was determined by direct sequence as described previously (Doyu *et al.*, 1992).

Data analysis

All variables were summarized using descriptive statistics, including median, mean, SD, percentile and percentages. Age at ADL milestone data from a sufficient number of the patients was evaluated by Kaplan–Meier analyses, and log rank test statistics were used to determine whether Kaplan–Meier transition curves differed among subgroups. Relationships between the age at each ADL milestone and the length of CAG repeat of *AR* gene were analysed using Pearson's correlation coefficient. Correlations between laboratory test value and the age at examination were also analysed using Pearson's correlation coefficient. *P*-values of <0.05 were considered to be statistically significant. Calculations were performed using the statistical software package Dr SPSS II for Windows (SPSS Japan Inc., Tokyo, Japan).

Results

Clinical and genetic backgrounds of SBMA patients

A total of 223 SBMA patients were included in this study (Table 1). All of the patients were of Japanese nationality. The mean age at the time of data collection was 55.2 ± 10.5 years (range = 30–87 years). The mean duration from onset assessed by the patient's initial awareness of muscle weakness was 9.8 ± 7.2 years (range = 0–37).

The mean number of CAG repeats in the *AR* gene was 46.6 ± 3.5 (range = 40–57). The location of the initial noticeable muscular weakness was lower extremities in 70.5%, upper extremities in 31.0%, bulbar symptoms in 11.4% and facial weakness in 2.4%. Some patients noticed muscle weakness initially in two locations simultaneously; thus overlap between the groups existed. Weakness in the lower extremities was noticed most often as difficulty in climbing stairs, followed by difficulty in walking for long distances and difficulty in standing from a sitting position. Bulbar symptoms were first noticed as a difficulty in articulating properly. ADL assessed by a modified Rankin scale at examination was 0–1 in 17.2%, 2–3 in 66.1% and 4–6 in 16.7% of the patients. Serum CK levels were 863.5 ± 762.5 IU/l (range = 31–4955; normal value = 45–245 IU/l), HbA1c levels were 5.7 ± 1.1% (range = 4.3–9.6; normal value = 4.3–5.8%), serum testosterone levels were 6.48 ± 1.83 ng/ml (range = 2.85–10.20; normal value = 2.7–10.7 ng/ml), serum AST levels were 44.3 ± 29.4 IU/l (range = 17–238; normal value = 0–41 IU/l), serum ALT levels were 52.6 ± 37.1 IU/l (range = 12–248; normal value = 0–45 IU/l) and serum total cholesterol levels were 219.3 ± 42.3 mg/dl (range = 119–413; normal value = 120–220 mg/dl).

Table 1 Clinical and genetic backgrounds of SBMA patients

Clinical and genetic features	Mean ± SD (range)
Age at examination (years)	55.2 ± 10.5 (30–87)
Duration from onset (years)[a]	9.8 ± 7.2 (0–37)
CAG-repeat length in *AR* gene (number)	46.6 ± 3.5 (40–57)
Location of initial muscular weakness the patients perceived (%)[b]	
Facial	2.4
Bulbar	11.4
Upper extremities	31.0
Lower extremities	70.5
Modified Rankin scale at examination (%)	
0–1	17.2
2–3	66.1
4–6	16.7
Serum markers at examination	
Serum CK (n = 182) (IU/l)	863.5 ± 762.5 (31–4955)
HbA1c level (n = 76) (%)	5.7 ± 1.1 (4.3–9.6)
Serum testosterone level (n = 61) (ng/ml)	6.48 ± 1.83 (2.85–10.20)
Serum AST (n = 130) (IU/l)	44.3 ± 29.4 (17–238)
Serum ALT (n = 133) (IU/l)	52.6 ± 37.1 (12–248)
Total cholesterol level (n = 82) (mg/dl)	219.3 ± 42.3 (119–413)

Normal values for serum CK range = 45–245 IU/l; HbA1c range = 4.3–5.8%; serum testosterone range = 2.7–10.7 ng/ml; serum AST range = 0–41 IU/l; serum ALT range = 0–45 IU/l; and total cholesterol range = 120–220 mg/dl. [a]Onset was assessed by patients' initial awareness of muscle weakness; [b]some patients noticed muscle weakness in two locations simultaneously.

Age at which ADL milestones appear

Age distributions at which the ADL milestones initially appeared are summarized in Fig. 1. Hand tremor was the earliest of the ADL milestones that the patients noticed, and it occurred at a median age of 33 years. Hand tremor was particularly noticed when patients used their hands such as in holding a drinking glass. Muscular weakness, predominantly in the lower extremities, was noticed at a median age of 44 years, followed by the need of a handrail when going up stairs at a median age of 49 years. Dysarthria, dysphagia and the use of a cane appeared at median ages of 50, 54 and 59 years, respectively. The use of a wheelchair started at a median age of 61 years. Patients developed pneumonia owing to aspiration and required in-hospital care at a median age of 62 years. The median age of those 15 patients who died before this report was 65 years. The predominant cause of death in eight of these cases was aspiration pneumonia. One patient died of lung cancer, and another patient died from ischaemic heart disease. One patient committed suicide. The causes of death of the other four patients were unknown. The ages of

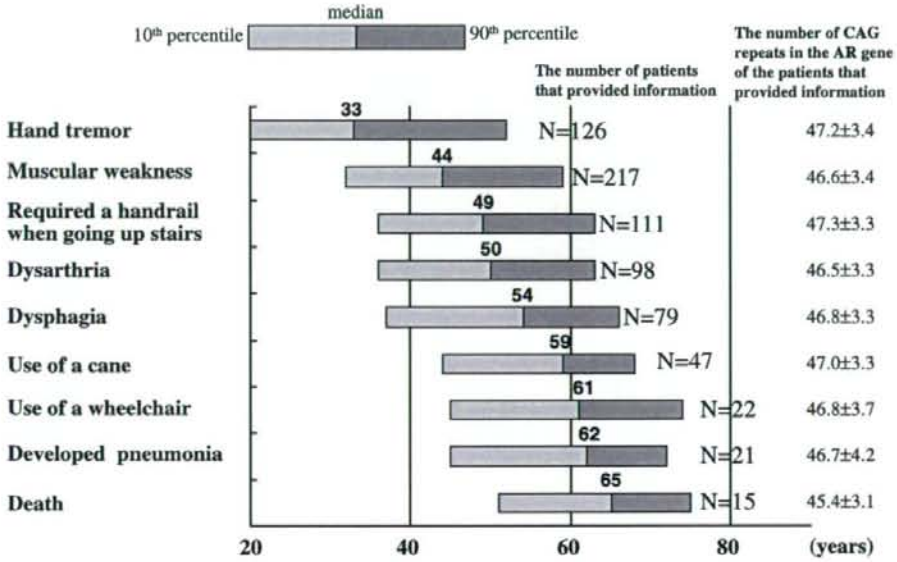

Fig. 1 Age distribution of ADL milestones for 223 SBMA patients. The mean number of CAG repeats in the *AR* gene of the patients does not differ significantly as shown at the right.

onset of each ADL milestone showed a considerable wide-ranged distribution from 25 to 30 years when assessed from the 10th to 90th percentile range. Although there were no significant differences in the mean number of CAG repeats in the *AR* gene of the patients in which we assessed the age at onset of each ADL milestone (Fig. 1), suggesting that age distributions at each milestone were derived from genetically uniform patients, we tested the hypothesis that the wide range in ages of onset at each milestone may be due to individual differences in CAG-repeat lengths.

Age at onset of each ADL milestone correlates well with CAG-repeat length

As shown in Fig. 2, the onset age of the individual ADL milestones examined showed significant correlations with the CAG-repeat length of the patients reporting on these symptoms ($r = -0.853$ to -0.447, $P < 0.016$–0.001). Of these, age at onset of hand tremor, requirement of a handrail, use of a wheelchair, developing pneumonia requiring in-hospital care and death were strongly correlated with the CAG repeats with $r < -0.5$. Furthermore, the onset ages of pneumonia and death were highly correlated with the CAG repeats with $r = -0.78$ and -0.85, respectively, indicating that these specific events, the onset ages of which the patients or their families were able to indicate more definitely, showed a more significant correlation with the CAG-repeat length than other ADL milestones.

Since 47 repeats was the median CAG-repeat length of the entire patient group, we further compared the Kaplan–Meier curves for age at onset of hand tremor, muscular weakness and requirement of a handrail between the patient group with 47 CAG repeats or more and those with <47 CAG repeats (Fig. 3). We assessed only these three ADL milestones, since the number of patients in these groups was sufficient to perform a log rank test analysis. The patients with <47 CAG repeats showed regression curves shifted by ~10 years compared with those with ≥47 CAG repeats (Fig. 3, $P < 0.001$ in log rank test). Together, these observations strongly suggest that the onset age of each ADL milestone is highly dependent on CAG-repeat length in the *AR* gene.

CAG-repeat length does not correlate with the rate of disease progression assessed by ADL milestones

In order to assess whether CAG-repeat length influences the disease progression rate, we examined the relationship between the time intervals from onset age of muscular weakness to that of requirement of a handrail when going up stairs, use of a cane, use of a wheelchair, development of pneumonia and death and the CAG-repeat lengths in these groups (Fig. 4). We did not find any significant correlations of the intervals among the onset age of the various milestones with the CAG-repeat length, suggesting that the progression rate of the disease is not significantly influenced by the CAG-repeat size.

In addition, we examined the declining regression assessed by those ADL milestones in individual patients with ≥47 CAG repeats compared with those with <47 (Fig. 5). These regression lines were divergent from each other, possibly because of divergent CAG-repeat size, while the mean slopes

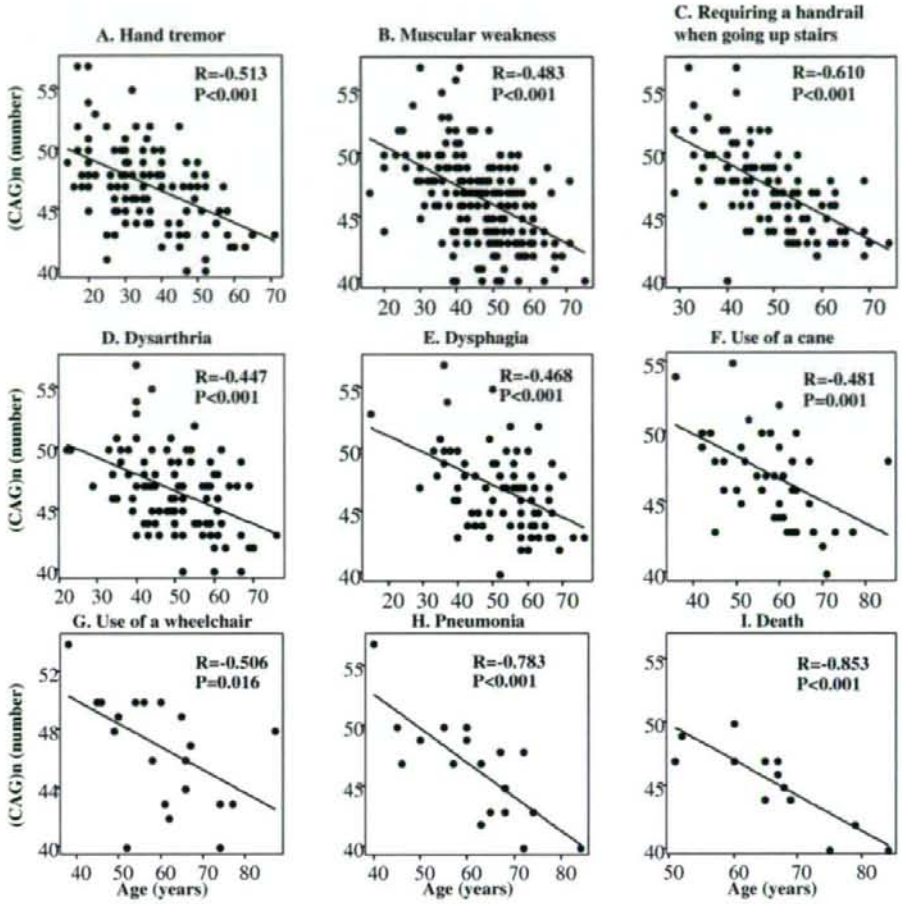

Fig. 2 (**A–I**) Correlation of the CAG-repeat number of and the age at each ADL milestone. There were significant correlations between CAG number and age at all milestones analysed using Pearson's correlation coefficient.

of the regression lines of the two groups were likely to be parallel. There were no significant differences between the interval times of the two groups as assessed by unpaired *t*-test (Fig. 5), suggesting, again, that the rate of disease progression was not markedly dependent upon the size of the CAG repeats.

Age-related changes of laboratory data and their relation to CAG repeats

Glucose intolerance, serum CK and ALT elevation and androgen insensitivity of SBMA patients have been reported (Sobue *et al.*, 1989; Shimada *et al.*, 1995; Dejager *et al.*, 2002; Sinnreich *et al.*, 2004). We examined the relationship between serum CK, HbA1c, testosterone, total cholesterol, AST and ALT levels and the age and CAG-repeat length of the patients. The serum levels of CK, AST and ALT were elevated in subpopulations of patients, particularly in the early phase of the disease, while these levels gradually declined with age (Fig. 6A, E and F). In advanced ages, the levels of these serum markers had declined to nearly normal levels. Serum testosterone levels were slightly elevated from control values in one-third of patients; in general, they declined slightly with age (Fig. 6C). However, even at these advanced ages testosterone levels were within or above the normal range. In contrast, HbA1c levels were within the normal range in the patients with short disease durations, but they gradually increased to above the normal range as the age of patients increased (Fig. 6B). Cholesterol levels were mildly elevated in some patients, but there was no particular age-dependent change observed (Fig. 6D). Elevated levels of these serum markers were not correlated with the CAG-repeat sizes (data not shown). Therefore, the levels of these markers appear to reflect the active pathological process of the disease, especially in the early or late phases, but their significance should be examined further.

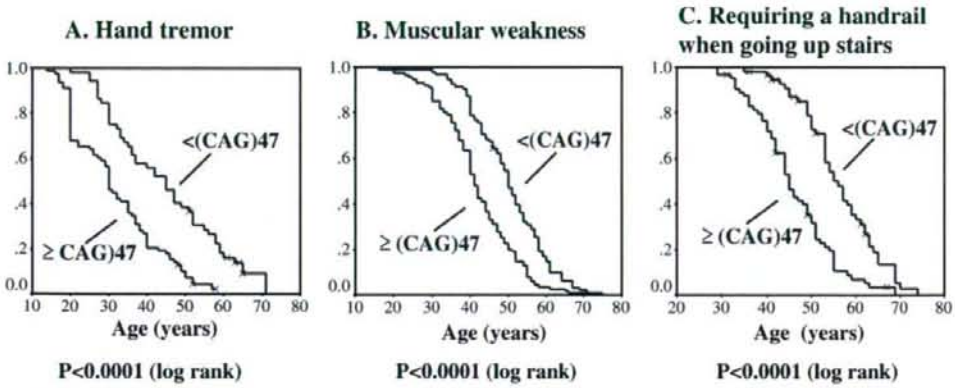

Fig. 3 (**A–C**) Kaplan–Meier analysis of age at onset of hand tremor, muscular weakness and requirement of a handrail. There was a highly significant difference between the patient group with ≥47 CAG repeats and the group with <47 CAG repeats, as compared by log rank tests.

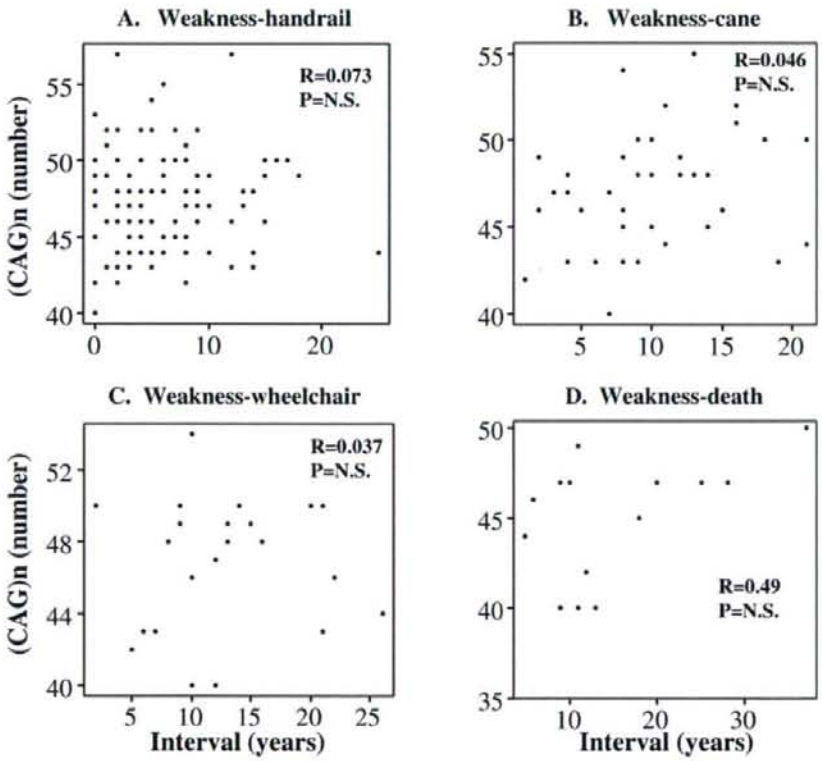

Fig. 4 (**A–D**) Correlation between the *AR* gene CAG number and the time interval between the ADL milestones. The time interval from the age at first awareness of muscular weakness to the age at requirement of a handrail, use of a cane, use of a wheelchair and death were compared with the CAG number by Pearson's correlation coefficient. There were no significant correlations in any of the interval times.

Discussion

Our study elucidated the natural history of SBMA patients based on nine ADL milestones. SBMA progressed slowly to the end stage with a median duration from onset assessed by muscle weakness to the appearance of pneumonia of 16 years, and to death of 22 years whereas the median durations from age of onset to the age of requirement of a handrail, dysarthria and dysphagia were 5, 6 and 10 years, respectively,

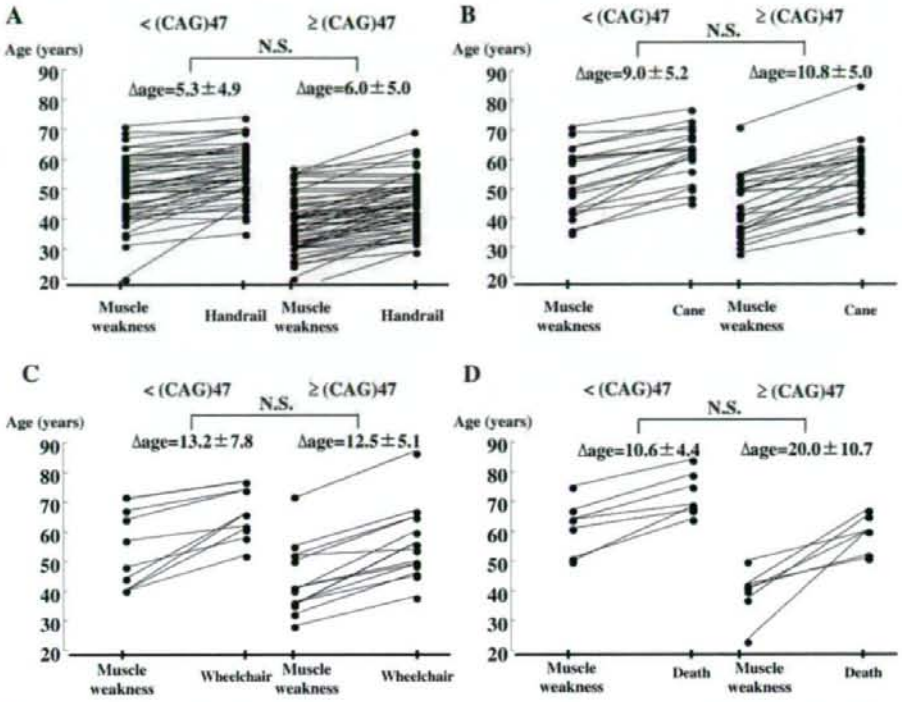

Fig. 5 (A–D) Individual case presentation of the declining regression assessed by ADL milestones. The interval times from the age at first awareness of weakness to the age at requirement of a handrail, use of a cane, use of a wheelchair and death are described for individual patients from two groups, those with <47 CAG repeats and those with ≥47 repeats. These regression lines were divergent from each other, possibly owing to divergent CAG-repeat size, while the mean slopes of the regression lines were likely to be parallel among the two subgroups of patients. There were no significant differences between the interval times of the two groups of patients analysed by unpaired *t*-test.

indicating that the ADL deterioration leading to a decline in the quality of daily living during early phases of the diseases is significant, in spite of a relatively long lifespan. The lifespan of SBMA patients was previously speculated to be 10–15 years shorter than those of the general Japanese male population (Mukai, 1989). In this study, 15 of the 223 patients died at a median age of 65 years. Although there are too few data to make a reliable calculation, this is ~12 years shorter than that of the current lifespan of the normal Japanese male indicated by the abridged life table announced by the Japanese Ministry of Health, Labor and Welfare in 2003, and, thus, is consistent with the previous speculation (Mukai, 1989). Of these 15 patients, the most common cause of death was pneumonia due to aspiration and dysphagia. Thus, the bulbar symptoms, such as difficulty in proper articulation and mild dysphagia, were relatively mild in their early manifestations, but were serious symptoms in the late phase of the disease, when the patients were prone to death. The progression was apparently slower than that of ALS, another adult-onset motoneuron disease, which occasionally mimics SBMA phenotypes, particularly in the early phase (La Spada *et al.*, 1992; Parboosingh *et al.*, 1997; Traynor *et al.*, 2000).

The onset ages of each ADL milestone were extremely variable, but all were well correlated with the CAG-repeat size in the AR gene. Patients with longer CAG-repeat sizes showed an earlier onset age of each ADL milestone examined, including occurrence of pneumonia or death in the end stage. Several previous studies also documented the natural history of SBMA. They showed that the age of disease onset assessed by muscle weakness was strongly correlated with *AR* gene CAG-repeat size (Doyu *et al.*, 1992; Igarashi *et al.*, 1992; La Spada *et al.*, 1992; Shimada *et al.*, 1995), whereas the onset ages of other symptoms such as fatigue, tremor, occurrence of gynaecomastia and severity of muscle weakness were not significantly correlated with repeat size (La Spada *et al.*, 1992; Amato *et al.*, 1993; Mariotti *et al.*, 2000; Dejager *et al.*, 2002; Sperfeld *et al.*, 2002). It is not clear why the relations between the onset age of these symptoms and CAG repeat size were not apparent in these reports, since significant correlations with the onset age of hand tremor and muscular weakness were confirmed in the present study. One possibility may be the relatively small sample sizes in the previous studies (Amato *et al.*, 1993; Sperfeld *et al.*, 2002). An alternative explanation may be that very early symptoms, such as

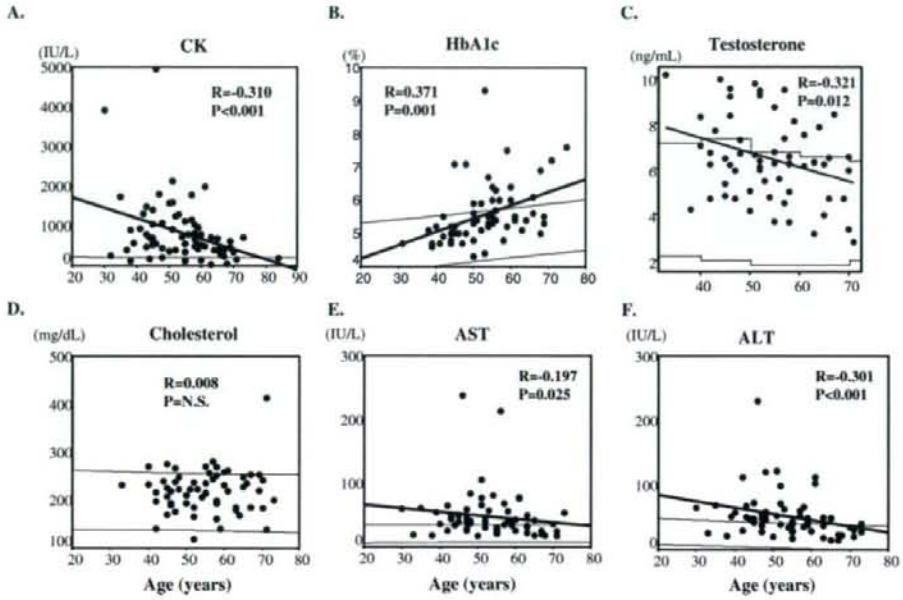

Fig. 6 (A–F) Correlation between the levels of serum markers and the age at examination. A weak, but significant, correlation was seen between HbA1c and age, while weak, but significant, inverse correlations were seen between CK, testosterone, AST and ALT and age as analysed by Pearson's correlation coefficient. Cholesterol levels were not correlated with age. The thin lines in each plot indicate the 95% confidence intervals calculated from control subjects.

gynaecomastia and fatigue, are not very accurate or reliable markers for ADL milestones compared with later symptoms, especially in a retrospective study. Indeed, the correlation of the onset age of tremor with CAG-repeat size was weaker than that of the onset age of the use of a wheelchair or a cane, which were more advanced ADL milestones used in our study.

The relationship between CAG-repeat size, disease markers and rate of disease progression have also been assessed extensively in Huntington's disease (Illarioshkin *et al.*, 1994; Brandt *et al.*, 1996; Furtado *et al.*, 1996; Penney *et al.*, 1997; Rosenblatt *et al.*, 2003). Neuronal loss in the caudate nucleus and putamen, adjusted for age of death, correlated well with CAG-repeat length (Furtado *et al.*, 1996; Penney *et al.*, 1997; Rosenblatt *et al.*, 2003). The rate of progression assessed by symptom severity controlled by duration from onset (Illarioshkin *et al.*, 1994) also correlated strongly with the CAG-repeat size. In addition, we previously demonstrated that the extent of cerebellar atrophy and severity of muscle weakness, both adjusted by age at examination correlated well with CAG-repeat size in SCA3 and SBMA, respectively (Doyu *et al.*, 1992; Abe *et al.*, 1998). These observations suggested that longer CAG repeats resulted in an earlier age at onset and greater neuronal loss when compared with shorter repeats. There is also some evidence that they contribute to a faster rate of clinical decline.

In our present study, as documented in Figs 2 and 3, patients with longer CAG repeats reached each of the ADL milestones such as hand tremor, muscle weakness or the requirement of a handrail when going up stairs much earlier than did the patients with shorter CAG repeats. Interestingly, however, the decline curves, as documented with Kaplan–Meier analyses, for these individual milestones were similar (Fig. 3), with an ~10-year difference between the patients with ≥47 repeats and those with <47 repeats. The earlier age at onset for each ADL milestone in patients with longer repeat lengths is similar to observations in cases of Huntington's disease.

The most striking observation in our study was that the interval periods between individual ADL milestones, such as between onset of muscle weakness and that of requirement of a handrail, use of a cane, being wheelchair-bound or death were not affected by the CAG-repeat length (Figs 4 and 5). Although patients with longer CAG-repeat size reached individual ADL milestones faster than those with shorter repeats, the decline rate from one ADL milestone to another was not influenced by the CAG-repeat size. These results suggest that the rate of disease progression assessed by ADL milestones is not influenced by CAG-repeat length.

Therefore, we may propose a view simulating the natural history of SBMA, in that, the decline curves of ADL in the SBMA patients with longer CAG-repeat size are shifted earlier than those in the SBMA patients with shorter CAG-repeat size, and the slopes of the decline curves are parallel to one another.

The phenotypic decline curves provided by mouse models of CAG-repeat diseases (Adachi *et al.*, 2003; von Horsten *et al.*, 2003) also support our view of the natural history of SBMA. The present findings are informative in understanding the pathophysiology of SBMA. CAG-repeat size is known to be a determinant factor for the entry of neuronal cells harbouring a mutant *AR* gene with expanded CAG repeats into the neuronal degeneration process *in vitro*, as well as *in vivo* (Mangiarini *et al.*, 1996). However, it is not known whether the rate of neuronal degeneration leading to subsequent cell death is dependent on CAG-repeat size. Once neuronal cell degeneration or neuronal cell dysfunction is initiated, the progression of degeneration to cell death may be determined by intrinsic factors such as a cell death processing system other than the CAG-repeat size. Thus, we suggest that the onset time of certain ADL milestones reflects how many neurons have entered into the neurodegeneration-dysfunction process, which is determined by CAG-repeat size, rather than the intrinsic cell death process.

Recently, we demonstrated that several interventions, anti-testosterone therapy with leuprorelin (Katsuno *et al.*, 2003), induction of Hsp70 (Adachi *et al.*, 2003; Katsuno *et al.*, 2005), inhibition of HDAC (Minamiyama *et al.*, 2004) or inhibition of Hsp90 (Waza *et al.*, 2005) showed potent therapeutic effects in improving the characteristic phenotypes and pathology in the SBMA transgenic mouse model. These observations strongly encourage the application of the therapeutics to human SBMA patients. Unlike the therapeutic approach commonly taken in neurodegenerative diseases of replacing lost substances such as neurotransmitters, these new therapeutics ameliorate the disease progression itself by preventing pathological molecular processes. Since the progression of SBMA is slow, clinical end-points will be useful for efficiently assessing the effectiveness of these therapies. The present study may indicate ADL milestones that can be clinical end-points in therapeutic trials. However, assessing the ADL milestones adopted in this study, such as the use of a cane or a wheelchair, would take years during clinical trials. Thus, we need to find a shorter-term surrogate marker that reflects the pathological process, although a genuine clinical therapeutic end-point should be examined to determine whether the ADL milestones are effectively delayed by the therapeutic intervention.

One interesting observation in this study is that serum testosterone levels were maintained at relatively high levels, even at advanced ages, although they did decrease with age (Fig. 6C). Since testosterone is an important triggering factor for polyglutamine-mediated motoneuron degeneration (Katsuno *et al.*, 2002, 2003), these findings suggest that anti-testosterone therapy with leuprorelin (Katsuno *et al.*, 2003) may be applicable even in aged SBMA patients.

The advantages of our study over previous studies are the large sample size and the employment of marked and apparent ADL milestones that the patients recognized easily. Nevertheless, several limitations are also present. One major limitation is that the study was retrospective in design and the decline curve was not successively and prospectively assessed in individual patients. A prospective study that follows individual patients in assessing the ADL milestones is needed to ascertain the validity of this natural history of SBMA.

The ADL milestones that we adopted for this study were selected with the assumption that they could be accurately assessed by us, the patients or family members, even in a retrospective study. However, as we demonstrated, the development of pneumonia and death showed higher significant correlations with CAG-repeat size than did other earlier ADL milestones such as the appearance of hand tremor or dysarthria, suggesting that these critical end-stage events may be more accurately assessed in a retrospective manner. We need further long-standing prospective studies to assess the disease progression more properly.

Acknowledgements

This study was supported by a COE grant from the Ministry of Education, Science and Sports of Japan and grants from the Ministry of Welfare, Health and Labor of Japan.

References

Abe Y, Tanaka F, Matsumoto M, Doyu M, Hirayama M, Kachi T, et al. CAG repeat number correlates with the rate of brainstem and cerebellar atrophy in Machado-Joseph disease. Neurology 1998; 51: 882–4.

Adachi H, Katsuno M, Minamiyama M, Sang C, Pagoulatos G, Angelidis C, et al. Heat shock protein 70 chaperone overexpression ameliorates phenotypes of the spinal and bulbar muscular atrophy transgenic mouse model by reducing nuclear-localized mutant androgen receptor protein. J Neurosci 2003; 23: 2203–11.

Adachi H, Katsuno M, Minamiyama M, Waza M, Sang C, Nakagomi Y, et al. Widespread nuclear and cytoplasmic accumulation of mutant androgen receptor in SBMA patients. Brain 2005; 128: 659–70.

Amato AA, Prior TW, Barohn RJ, Snyder P, Papp A, Mendell JR. Kennedy's disease: a clinicopathologic correlation with mutations in the androgen receptor gene. Neurology 1993; 43: 791–4.

Andrew SE, Goldberg YP, Kremer B, Telenius H, Theilmann J, Adam S, et al. The relationship between trinucleotide (CAG) repeat length and clinical features of Huntington's disease. Nat Genet 1993; 4: 398–403.

Brandt J, Bylsma FW, Gross R, Stine OC, Ranen N, Ross CA. Trinucleotide repeat length and clinical progression in Huntington's disease. Neurology 1996; 46: 527–31.

Dejager S, Bry-Gauillard H, Bruckert E, Eymard B, Salachas F, LeGuern E, et al. A comprehensive endocrine description of Kennedy's disease revealing androgen insensitivity linked to CAG repeat length. J Clin Endocrinol Metab 2002; 87: 3893–901.

Doyu M, Sobue G, Mukai E, Kachi T, Yasuda T, Mitsuma T, et al. Severity of X-linked recessive bulbospinal neuronopathy correlates with size of the tandem CAG repeat in androgen receptor gene. Ann Neurol 1992; 32: 707–10.

Furtado S, Suchowersky O, Rewcastle B, Graham L, Klimek ML, Garber A. Relationship between trinucleotide repeats and neuropathological changes in Huntington's disease. Ann Neurol 1996; 39: 132–6.

Igarashi S, Tanno Y, Onodera O, Yamazaki M, Sato S, Ishikawa A, et al. Strong correlation between the number of CAG repeats in androgen receptor genes and the clinical onset of features of spinal and bulbar muscular atrophy. Neurology 1992; 42: 2300–2.

Illarioshkin SN, Igarashi S, Onodera O, Markova ED, Nikolskaya NN, Tanaka H, et al. Trinucleotide repeat length and rate of progression of Huntington's disease. Ann Neurol 1994; 36: 630–5.

Iwamoto T, Yanase T, Koh E, Horie H, Baba K, Namiki M, et al. Reference ranges of serum total and free testosterone in Japanese male adults. Nihon Hinyoukigakkai Zassi (in Japanese) 2004; 95: 751–60.

Katsuno M, Adachi H, Kume A, Li M, Nakagomi Y, Niwa H, et al. Testosterone reduction prevents phenotypic expression in a transgenic mouse model of spinal and bulbar muscular atrophy. Neuron 2002; 35: 843–54.

Katsuno M, Adachi H, Doyu M, Minamiyama M, Sang C, Kobayashi Y, et al. Leuprorelin rescues polyglutamine-dependent phenotypes in a transgenic mouse model of spinal and bulbar muscular atrophy. Nat Med 2003; 9: 768–73.

Katsuno M, Sang C, Adachi H, Minamiyama M, Waza M, Tanaka F, et al. Pharmacological induction of heat-shock proteins alleviates polyglutamine-mediated motor neuron disease. Proc Natl Acad Sci USA 2005; 102: 16801–6.

Kennedy WR, Alter M, Sung JH. Progressive proximal spinal and bulbar muscular atrophy of late onset. A sex-linked recessive trait. Neurology 1968; 18: 671–80.

Koide R, Ikeuchi T, Onodera O, Tanaka H, Igarashi S, Endo K, et al. Unstable expansion of CAG repeat in hereditary dentatorubral-pallidoluysian atrophy (DRPLA). Nat Genet 1994; 6: 9–13.

La Spada AR, Wilson EM, Lubahn DB, Harding AE, Fischbeck KH. Androgen receptor gene mutations in X-linked spinal and bulbar muscular atrophy. Nature 1991; 352: 77–9.

La Spada AR, Roling DB, Harding AE, Warner CL, Spiegel R, Hausmanowa-Petrusewicz I, et al. Meiotic stability and genotype-phenotype correlation of the trinucleotide repeat in X-linked spinal and bulbar muscular atrophy. Nat Genet 1992; 2: 301–4.

Li M, Miwa S, Kobayashi Y, Merry DE, Yamamoto M, Tanaka F, et al. Nuclear inclusions of the androgen receptor protein in spinal and bulbar muscular atrophy. Ann Neurol 1998a; 44: 249–54.

Li M, Nakagomi Y, Kobayashi Y, Merry DE, Tanaka F, Doyu M, et al. Nonneural nuclear inclusions of androgen receptor protein in spinal and bulbar muscular atrophy. Am J Pathol 1998b; 153: 695–701.

Lund A, Udd B, Juvonen V, Andersen PM, Cederquist K, Davis M, et al. Multiple founder effects in spinal and bulbar muscular atrophy (SBMA, Kennedy disease) around the world. Eur J Hum Genet 2001; 9: 431–6.

Mangiarini L, Sathasivam K, Seller M, Cozens B, Harper A, Hetherington C, et al. Exon 1 of the HD gene with an expanded CAG repeat is sufficient to cause a progressive neurological phenotype in transgenic mice. Cell 1996; 87: 493–506.

Mariotti C, Castellotti B, Pareyson D, Testa D, Eoli M, Antozzi C, et al. Phenotypic manifestations associated with CAG-repeat expansion in the androgen receptor gene in male patients and heterozygous females: a clinical and molecular study of 30 families. Neuromuscul Disord 2000; 10: 391–7.

Minamiyama M, Katsuno M, Adachi H, Waza M, Sang C, Kobayashi Y, et al. Sodium butyrate ameliorates phenotypic expression in a transgenic mouse model of spinal and bulbar muscular atrophy. Hum Mol Genet 2004; 13: 1183–92.

Mukai E. Clinical features of bulbo-spinal muscular atrophy. Shinkeinaika (in Japanese) 1989; 30: 1–7.

Parboosingh JS, Figlewicz DA, Krizus A, Meininger V, Azad NA, Newman DS, et al. Spinobulbar muscular atrophy can mimic ALS: the importance of genetic testing in male patients with atypical ALS. Neurology 1997; 49: 568–72.

Penney JB Jr, Vonsattel JP, MacDonald ME, Gusella JF, Myers RH. CAG repeat number governs the development rate of pathology in Huntington's disease. Ann Neurol 1997; 41: 689–92.

Rosenblatt A, Abbott MH, Gourley LM, Troncoso JC, Margolis RL, Brandt J, et al. Predictors of neuropathological severity in 100 patients with Huntington's disease. Ann Neurol 2003; 54: 488–93.

Sasaki H, Fukazawa T, Yanagihara T, Hamada T, Shima K, Matsumoto A, et al. Clinical features and natural history of spinocerebellar ataxia type 1. Acta Neurol Scand 1996; 93: 64–71.

Shimada N, Sobue G, Doyu M, Yamamoto K, Yasuda T, Mukai E, et al. X-linked recessive bulbospinal neuronopathy: clinical phenotypes and CAG repeat size in androgen receptor gene. Muscle Nerve 1995; 18: 1378–84.

Sinnreich M, Sorenson EJ, Klein CJ. Neurologic course, endocrine dysfunction and triplet repeat size in spinal bulbar muscular atrophy. Can J Neurol Sci 2004; 31: 378–82.

Sobue G, Hashizume Y, Mukai E, Hirayama M, Mitsuma T, Takahashi A. X-linked recessive bulbospinal neuronopathy. A clinicopathological study. Brain 1989; 112: 209–32.

Sperfeld AD, Karitzky J, Brummer D, Schreiber H, Haussler J, Ludolph AC, et al. X-linked bulbospinal neuronopathy: Kennedy disease. Arch Neurol 2002; 59: 1921–6.

Tanaka F, Reeves MF, Ito Y, Matsumoto M, Li M, Miwa S, et al. Tissue-specific somatic mosaicism in spinal and bulbar muscular atrophy is dependent on CAG-repeat length and androgen receptor-gene expression level. Am J Hum Genet 1999; 65: 966–73.

Traynor BJ, Codd MB, Corr B, Forde C, Frost E, Hardiman O. Amyotrophic lateral sclerosis mimic syndromes: a population-based study. Arch Neurol 2000; 57: 109–13.

van Swieten JC, Koudstaal PJ, Visser MC, Schouten HJ, van Gijn J. Interobserver agreement for the assessment of handicap in stroke patients. Stroke 1988; 19: 604–7.

von Horsten S, Schmitt I, Nguyen HP, Holzmann C, Schmidt T, Walther T, et al. Transgenic rat model of Huntington's disease. Hum Mol Genet 2003; 12: 617–24.

Waza M, Adachi H, Katsuno M, Minamiyama M, Sang C, Tanaka F, et al. 17-AAG, an Hsp90 inhibitor, ameliorates polyglutamine-mediated motor neuron degeneration. Nat Med 2005; 11: 1088–95.

Review

The proteasome: Overview of structure and functions

By Keiji TANAKA*1,†

(Communicated by Takao SEKIYA, M.J.A.)

Abstract: The proteasome is a highly sophisticated protease complex designed to carry out selective, efficient and processive hydrolysis of client proteins. It is known to collaborate with ubiquitin, which polymerizes to form a marker for regulated proteolysis in eukaryotic cells. The highly organized proteasome plays a prominent role in the control of a diverse array of basic cellular activities by rapidly and unidirectionally catalyzing biological reactions. Studies of the proteasome during the past quarter of a century have provided profound insights into its structure and functions, which has appreciably contributed to our understanding of cellular life. Many questions, however, remain to be elucidated.

Keywords: proteasome, ubiquitin, intracellular proteolysis, multisubunit complex, molecular chaperone

Introduction

The proteasome is a large protein complex responsible for degradation of intracellular proteins, a process that requires metabolic energy. Polymerization of ubiquitin, a key molecule known to work in concert with the proteasome, serves as a degradation signal for numerous target proteins; the destruction of a protein is initiated by covalent attachment of a chain consisting of several copies of ubiquitin (more than four ubiquitin molecules), through the concerted actions of a network of proteins, including the E1 (ubiquitin-activating), E2 (ubiquitin-conjugating) and E3 (ubiquitin-ligating) enzymes.[1),2)] The polymerized ubiquitin chain acts as a signal that shuttles the target proteins to the proteasome, where the substrate is proteolytically broken down. For accurate selection of the proteins, numerous enzymes (e.g., 2 E1 proteins, approximately 30 E2 proteins and more than 500 different species of E3 in humans) are mobilized with this cascade system. The set of E3 proteins is highly diverse, because each E3 enzyme usually selectively recognizes a protein substrate for ubiquitylation. Furthermore, it should be noted that ubiquitylation is a reversible reaction, because many cysteine-protease and metalloprotease deubiquitylating enzymes (DUBs) are present in the cell. Interestingly, the human genome encodes approximately 95 putative DUBs.[3)] Certain DUBs are responsible for the maturation of ubiquitin from its precursor proteins and products of genes that encode polyubiquitin or ubiquitin fused with ribosomal proteins. Other DUBs function at the initial stage during the breakdown of ubiquitin-tagged proteins to allow ubiquitins to be recycled. The ubiquitin–proteasome system (UPS) controls almost all basic cellular processes—such as progression through the cell cycle, signal transduction, cell death, immune responses, metabolism, protein quality control and development—by degrading short-lived regulatory or structurally aberrant proteins.[4)–6)] The divergent roles of the UPS have been reported in detail and reviewed comprehensively.[1)–6)] In this review, I provide an overview of the structure and functions of uniquely specified proteasomes. Due to space limitations, I have primarily cited review articles with the exception of particularly important or recently published papers.

1. 26S and 30S Proteasomes

The proteasome is made up of two subcom-

*1 Laboratory of Frontier Science, Tokyo Metropolitan Institute of Medical Science, Tokyo, Japan.
† Correspondence should be addressed: K. Tanaka, Laboratory of Frontier Science, Tokyo Metropolitan Institute of Medical Science, 3-18-22, Honkomagome, Bunkyo-ku, Tokyo 113-8613, Japan (e-mail: tanaka-kj@igakuken.or.jp).

doi: 10.2183/pjab/85.12

Table 1. Subtypes of proteasomes and their regulators

	Other nomenclature
Catalytic 20S Proteasomes	
Standard (or Constitutive) Proteasome	20S Core Particle (CP)
Immunoproteasome	
Thymoproteasome	
Testis-specific Proteasome	
Regulators	
PA700	19S Regulatory Particle (RP)
PA200	Blm10
PA28$\alpha\beta$	11S Regulator (REG)
PA28γ	
Active Proteasomes	
PA700–CP–PA700 (19S–20S–19S)	30S Proteasome
PA700–CP (19S–20S)	26S Proteasome
PA200–CP–PA200	
PA200–CP	
PA28$\alpha\beta$–CP–PA28$\alpha\beta$ (11S–20S–11S)	
PA28$\alpha\beta$–CP*	
PA28$\alpha\beta$–CP–PA700	Hybrid Proteasome
PA28γ–CP–PA28γ	
PA28γ–CP*	
PA28γ–CP–PA700*	
PA200–CP–PA700**	
PA28$\alpha\beta$–CP–PA200*	
PA28γ–CP–PA200*	

*unidentified complex; **referred to as alternative hybrid proteasome

plexes: a catalytic core particle (CP; also known as the 20S proteasome) and one or two terminal 19S regulatory particle(s) (RP) that serves as a proteasome activator with a molecular mass of approximately 700 kDa (called PA700) (Table 1).[7)–9)] The 19S RP binds to one or both ends of the latent 20S proteasome to form an enzymatically active proteasome. The apparent sedimentation coefficient of the active proteasome as determined by density-gradient centrifugation analysis is 26S and accordingly the complex is usually referred to as the 26S proteasome. Physicochemical analysis, however, has revealed that the correct sedimentation coefficient is approximately 30S.[10)] The size difference is probably due to the attachment of one 19S RP to the 20S proteasome to form the so-called 26S proteasome, whereas the elongated 30S molecule, which is likely the functional unit in the cell, may include a pair of symmetrically disposed 19S RPs that are attached to both ends of the central portion of the complex (Fig. 1). In this article, however, I will primarily use 26S proteasome without distinguishing between these two forms of the proteasome, unless otherwise specified.

As mentioned above, the 26S proteasome is a 2.5-MDa multicatalytic degradation machine that contains a 20S CP and one or two 19S RPs, which associate with the termini of the barrel-shaped central particle. The 19S RP serves to recognize ubiquitylated client proteins and is thought to play a role in their unfolding and translocation into the interior of the 20S CP, which contains catalytic

Abbreviations:
aa: amino acids
AAA-ATPase: ATPase associated with diverse cellular activities
AIRAP: arsenite-inducible proteasomal 19S regulatory-associated protein
AIRAPL: AIRAP-like gene
CD: cluster of differentiation
CP: core particle
cTECs: cortical thymic epithelial cells
CTL: cytotoxic T lymphocyte
DSBs: double strand breaks
DUB: deubiquitylating enzyme
EM: electron microscopy
FDA: Food and drug administration
GFP: green fluorescent protein
HbYX: hydrophobic-tyrosine-X
HCV: hepatitis C virus
IFN: interferon
MG-132: *N*-carbobenzoxy-leu-leu-leucinal
MHC: major histocompatibility complex
NER: nuclear excision repair
Ntn: N-terminal nucleophile
PA: proteasome activator
PAC: proteasome assembling chaperone
PGPH: peptidylglutamyl-peptide hydrolyzing
PI: proteasome inhibitor
PIP: proteasome-interacting protein
POMP: proteasome maturation protein
PSI: *N*-carbobenzoxy-L-gamma-t-butyl-L-glutamyl-L-alanyl-L-leucinal
REG: 11S regulator
RP: regulatory particle
siRNA: small interfering RNA
TAP: transporter associated with antigen processing
TCR: T cell receptor
TOP: thimet oligopeptidase
UBA: ubiquitin-associated
UBL: ubiquitin-like
UPS: ubiquitin–proteasome system
Z-L_3VS: carboxybenzyl-leucyl-leucyl-leucine vinyl sulfone

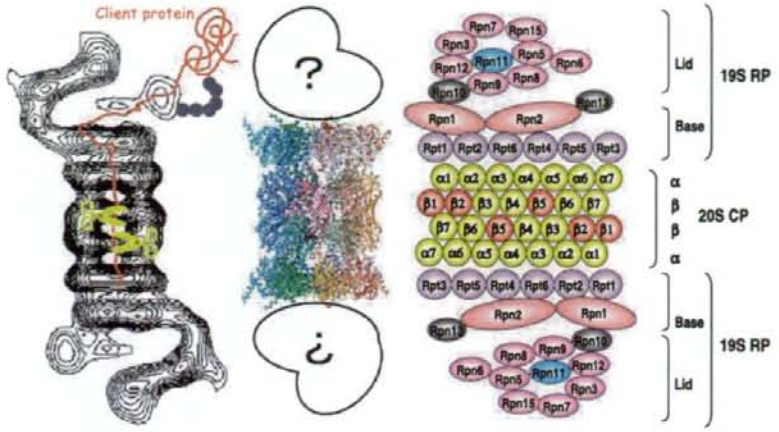

Fig. 1. Schematic diagram of the 26S proteasome. Left panel: Averaged image of the rat 26S proteasome complex based on electron micrographs. Photograph kindly provided by W. Baumeister. U, ubiquitin. Middle panel: The overall tertiary structure of the bovine 20S proteasome (central portion); the structures of the 19S RPs have not yet been determined (the pair of symmetrically disposed terminal structures depicted by question marks). Right panel: Schematic drawing of the subunit structure. CP, core particle (20S proteasome); RP, 19S regulatory particle consisting of the base and lid subcomplexes; Rpn, RP non-ATPase; Rpt, RP triple-ATPase.

threonine residues on the surface of a chamber formed by two β-rings.

2. The CP or 20S Proteasome

The 20S CP (alias 20S proteasome) is well characterized structurally (Fig. 1). It is a well-organized protein complex with a sedimentation coefficient of 20S and a molecular mass of approximately 750 kDa. When viewed electron microscopically, the 20S proteasome appears as a cylinder-like structure in various eukaryotes, including yeast and mammals. It forms a packed particle, a result of axial stacking of two outer α-rings and two inner β-rings, which are made up of seven structurally similar α and β subunits, respectively; the rings form an $\alpha_{1\text{-}7}\beta_{1\text{-}7}\beta_{1\text{-}7}\alpha_{1\text{-}7}$ structure. The 20S proteasome plays essentially the same proteolytic roles in all eukaryotes, differing from proteasomes in prokaryotes that mainly consists of homo-hepatmeric α- and β-rings of the same α and β subunits, respectively, i.e., the $\alpha\beta\beta\alpha$ structure.[8),11)] Accordingly, the overall structures and functions of the individual subunits are highly conserved among eukaryotic species, except for a specialized form(s) that is associated with adaptive immune responses, which will be described in a later section. Indeed, the yeast (*Saccharomyces cerevisiae*) and mammalian (bovine) 20S proteasomes are characterized by the same highly ordered, quaternary structures, as demonstrated by X-ray crystallography.[12),13)] The subunits of the 20S proteasome are specifically located within the complex with C2 symmetry. These subunits are listed in Table 2.

The three β-type subunits of each inner ring contain catalytically active threonine residues at their N termini and show N-terminal nucleophile (Ntn) hydrolase activity, indicating that the proteasome is a threonine protease that does not fall into the known seryl, thiol, carboxyl and metalloprotease families. The β1, β2 and β5 subunits are associated with caspase-like/PGPH (peptidylglutamyl-peptide hydrolyzing), trypsin-like and chymotrypsin-like activities, respectively, which confer the ability to cleave peptide bonds at the C-terminal side of acidic, basic and hydrophobic amino-acid residues, respectively. Two pairs of these three active sites face the interior of the cylinder and reside in a chamber formed by the centers of the abutting β-rings. The crystal structure of the 20S proteasome reveals that the center of the α-ring is almost completely closed, preventing proteins from penetrating into the inner chamber of the β-ring that contains the proteolytically active sites. Moreover, the N termini of the α subunits

Table 2. Proteasome subunits and proteasome-interacting proteins (PIPs) known to function as auxiliary factors

Category	Subclassification	Systematic nomenclature	HUGO	Miscellaneous nomenclature		human (yeast) amino acids	Motif	Lethality	Function
				Human	Yeast (budding/fission)				
20S CP	α type	α1	PSMA6	iota	SCL1, YC7	(252) 246	NLS	+	
	subunits	α2	PSMA2	C3	PRE8, Y7	(250) 233	NLS	+	
		α3	PSMA4	C9	PRE9, Y13	(258) 261	NLS	−	
		α4	PSMA7	C6	PRE6	(254) 248	NLS	+	
		α5	PSMA5	zeta	PUP2, DOA5	(260) 241		+	
		α6	PSMA1	C2	PRE5	(234) 263		+	
		α7	PSMA3	C8	PRE10, YC1	(288) 254		+	
		α8	PSMA8		—	256			
	β type	β1	PSMB6	Y, delta	PRE3	(19+196) 34+205	Ntn	+	Caspase-like
	subunits	β2	PSMB7	Z	PUP1	(29+232) 43+234	Ntn	+	Trypsin-like
		β3	PSMB3	C10	PUP3	(205) 205		+	
		β4	PSMB2	C7	PRE1	(198) 201		+	
		β5	PSMB5	X, MB1, epsilon	PRE2, DOA3	(75+212) 59+204	Ntn	+	Chymotrypsin-like
		β6	PSMB1	C5	PRE7	(19+222) 28+213		+	
		β7	PSMB4	N3, beta	PRE4	(33+233) 45+219		+	
		β1i	PSMB9	LMP2, RING12	—	20+199	Ntn	(−)	Caspase-like
		β2i	PSMB10	MECL1, LMP10	—	39+234	Ntn	(−)	Trypsin-like
		β5i	PSMB8	LMP7, RING10	—	72+204	Ntn	(−)	Chymotrypsin-like
		β5t	PSMB11		—	44+251	Ntn	(−)	Chymotrypsin-like
PA700	ATPase	Rpt1	PSMC2	S7, Mss1	YTA3, CIM5	(467) 433	AAA	+	ATPase
(19S RP)	subunits	Rpt2	PSMC1	S4, p56	YTA5/mts2	(437) 440	AAA, HbYX	+ (−)	ATPase, Gate-opning
		Rpt3	PSMC4	S6, Tbp7, P48	YTA2	(428) 418	AAA, HbYX	+ (+)	ATPase, Gate-opning
		Rpt4	PSMC6	S10b, p42	SUG2, PCS1, CRL13	(437) 389	AAA	+	ATPase
		Rpt5	PSMC3	S6′, Tbp1	YTA1	(434) 439	AAA, HbYX	+ (+)	ATPase, Gate-opning
		Rpt6	PSMC5	S8, p45, Trip1	SUG1, CRL3, CIM3/let1	(405) 406	AAA	+	ATPase
	non-ATPase	Rpn1	PSMD2	S2, p97	HRD2, NAS1/mts4	(993) 908	PC	+	PIPs scaffold
	subunits	Rpn2	PSMD1	S1, p112	SEN3	(945) 953	PC, NLS	+	PIPs scaffold
		Rpn3	PSMD3	S3, p58	SUN2	(523) 534	PCI, PAM	+	
		Rpn5	PAMD12	p55	NAS5	(445) 456	PCI	+	
		Rpn6	PSMD11	S9, p44.5	NAS4	(434) 422	PCI, PAM	+	
		Rpn7	PSMD6	S10a, P44		(429) 389	PCI	+	
		Rpn8	PSMD7	S12, p40, MOV34	NAS3	(338) 324	MPN	+	
		Rpn9	PSMD13	S11, p40.5	NAS7/mts1	(393) 376	PCI	−	

Continued to the next page.